CellPress
PARTNER JOURNAL

Molecular Plant
Resource Article

A Resource for Inactivation of MicroRNAs Using Short Tandem Target Mimic Technology in Model and Crop Plants

Ting Peng[1,2,3,17], Mengmeng Qiao[3,17], Haiping Liu[3,17], Sachin Teotia[1,3,16,17], Zhanhui Zhang[1,3,17], Yafan Zhao[1,2], Bobo Wang[1,2], Dongjie Zhao[3], Lina Shi[1,3], Cui Zhang[4], Brandon Le[4], Kestrel Rogers[4], Chathura Gunasekara[5], Haitang Duan[6], Yiyou Gu[3], Lei Tian[1,3], Jinfu Nie[7,8,9], Jian Qi[7,8], Fanrong Meng[1,3], Lan Huang[10], Qinghui Chen[3,11], Zhenlin Wang[6], Jinshan Tang[12], Xiaoqing Tang[3], Ting Lan[13], Xuemei Chen[4,13,*], Hairong Wei[5,14,*], Quanzhi Zhao[1,2,*] and Guiliang Tang[1,3,13,15,*]

[1]Collaborative Innovation Center of Henan Grain Crops, Henan Agricultural University, Zhengzhou 450002, China

[2]Key Laboratory of Rice Biology in Henan Province, Henan Agricultural University, Zhengzhou 450002, China

[3]Department of Biological Sciences, Life Science and Technology Institute, Michigan Technological University, Houghton, MI 49931, USA

[4]Department of Botany and Plant Sciences, Institute of Integrative Genome Biology, University of California, Riverside, CA 92521, USA

[5]School of Forest Resources and Environmental Science, Life Science and Technology Institute, Michigan Technological University, Houghton, MI 49931, USA

[6]Department of Computer Science, Michigan Technological University, Houghton, MI 49931, USA

[7]Anhui Province Key Laboratory of Medical Physics and Technology, Center of Medical Physics and Technology, Hefei Institutes of Physical Science, Chinese Academy of Sciences, Hefei, Anhui, China

[8]Hefei Cancer Hospital, Chinese Academy of Sciences, Hefei, Anhui, China

[9]Guangzhou Institute of Biomedicine and Health, Chinese Academy of Sciences, Guangzhou, China

[10]College of Information and Electrical Engineering, China Agricultural University, Beijing 100083, China

[11]Department of Kinesiology and Integrative Physiology, Life Science and Technology Instituted, Michigan Technological University, Houghton, MI 49931, USA

[12]School of Technology, Michigan Technological University, Houghton, MI 49931, USA

[13]Guangdong Provincial Key Laboratory for Plant Epigenetics, College of Life Sciences and Oceanography, Shenzhen University, Shenzhen 518060, P.R. China

[14]Beijing Advanced Innovation Center for Tree Breeding by Molecular Design, Beijing Forestry University, Beijing 100083, P.R. China

[15]Key Laboratory of Plant Stress Biology, State Key Laboratory of Cotton Biology, School of Life Sciences, Henan University, Kaifeng 475004, China

[16]Present address: Department of Biotechnology, Sharda University, Greater Noida, 201306, India

[17]These authors contributed equally to this article.

***Correspondence: Guiliang Tang (gtang1@mtu.edu), Quanzhi Zhao (qzzhaoh@126.com), Hairong Wei (hairong@mtu.edu), Xuemei Chen (xuemei.chen@ucr.edu)**

https://doi.org/10.1016/j.molp.2018.09.003

ABSTRACT

microRNAs (miRNAs) are endogenous small non-coding RNAs that bind to mRNAs and target them for cleavage and/or translational repression, leading to gene silencing. We previously developed short tandem target mimic (STTM) technology to deactivate endogenous miRNAs in *Arabidopsis*. Here, we created hundreds of STTMs that target both conserved and species-specific miRNAs in *Arabidopsis*, tomato, rice, and maize, providing a resource for the functional interrogation of miRNAs. We not only revealed the functions of several miRNAs in plant development, but also demonstrated that tissue-specific inactivation of a few miRNAs in rice leads to an increase in grain size without adversely affecting overall plant growth and development. RNA-seq and small RNA-seq analyses of STTM156/157 and STTM165/166 transgenic plants revealed the roles of these miRNAs in plant hormone biosynthesis and activation, secondary metabolism, and ion-channel activity-associated electrophysiology, demonstrating that STTM technology is an effective approach for studying miRNA functions. To facilitate the study and application of STTM transgenic plants and to provide a useful platform for storing and sharing of information about miRNA-regulated gene networks, we have established an online Genome Browser (https://blossom.ffr.mtu.edu/designindex2.php) to display the transcriptomic and miRNAomic changes in STTM-induced miRNA knockdown plants.

Published by the Molecular Plant Shanghai Editorial Office in association with Cell Press, an imprint of Elsevier Inc., on behalf of CSPB and IPPE, SIBS, CAS.

Key words: short tandem target mimic (STTM), miRNA, RNA-seq, *Arabidopsis*, crop

Peng T., Qiao M., Liu H., Teotia S., Zhang Z., Zhao Y., Wang B., Zhao D., Shi L., Zhang C., Le B., Rogers K., Gunasekara C., Duan H., Gu Y., Tian L., Nie J., Qi J., Meng F., Huang L., Chen Q., Wang Z., Tang J., Tang X., Lan T., Chen X., Wei H., Zhao Q., and Tang G. (2018). A Resource for Inactivation of MicroRNAs Using Short Tandem Target Mimic Technology in Model and Crop Plants. Mol. Plant. **11**, 1400–1417.

INTRODUCTION

The discovery of microRNAs (miRNAs) has enriched our understanding of the complexity of gene regulatory networks (Li et al., 2014). This complexity is reflected by the fact that large miRNA families in plants and animals have many members with redundant functions (Tang, 2010; Fromm et al., 2015; Cui et al., 2016). Owing to the partially overlapping roles of different temporospatially expressed miRNA members, functional studies of a specific miRNA family can be best achieved through simultaneous knockdown of all miRNAs in a family (Teotia et al., 2016). Such technology came into being with the discovery of a target mimic (TM), *INDUCED BY PHOSPHATE STARVATION1* (*IPS1*), in *Arabidopsis* (Franco-Zorrilla et al., 2007), and was further developed into a powerful technology termed short tandem target mimic (STTM) (Yan et al., 2012). TMs, based upon *IPS1*-derived structures, are long (~500 nt) and have three central mismatches in the miRNA binding site; these TMs can be used to sequester any miRNA of interest, leading to loss of function. Some highly abundant miRNAs such as miR165/166 cannot be efficiently silenced by TMs, and expression of miR165/166 TMs in transgenic plants results in a weak phenotype. TMs have been used to knock down the expression of many target miRNAs in *Arabidopsis* and have revealed the roles of miRNAs in morphology and development. Examples include the involvement of miR156 and miR172 in flowering; miR164, miR319, miR393, and miR394 in leaf shape; miR164 and miR159 in overall plant development; miR170/171 in leaf color; miR169 in rosette size; and miR167 in seed development, among others (Franco-Zorrilla et al., 2007; Todesco et al., 2010). Many researchers subsequently used these as well as other TMs to decipher and uncover the other roles of these miRNAs and also of miRNAs for which knockdown did not result in any visible phenotype.

Another technology to block miRNA functions in animal cells, termed molecular sponges (SPs), has recently been applied in *Arabidopsis* (Ebert et al., 2007; Reichel et al., 2015). In contrast to the SPs, used to block miRNAs in animal cells, which contain only four copies of cleavage-resistant miRNA binding sites (Ebert et al., 2007), the SPs used in *Arabidopsis* contain up to 15 copies of them (Reichel et al., 2015) . SPs have been used to silence miR165/166, miR159, miR164, and miR390 in *Arabidopsis* (Reichel et al., 2015).

STTMs are about 100 nt in length and contain two miRNA binding elements (such as two TMs in tandem) with a mismatch at the miRNA cleavage site, spaced by a weak stem-loop linker of 48–88 nt. STTM induces the degradation of most, if not all, cognate miRNAs, partly through the action of small degrading nucleases (Yan et al., 2012). STTMs have been successfully applied to silence numerous miRNA families in *Arabidopsis* (Yan et al., 2012) and in a few staple crops and model plants, including tomato (Jia et al., 2015; Jiang et al., 2018), rice (Zhang et al., 2017a, 2018), wheat (Guo et al., 2018), tobacco (Sha et al., 2014), Medicago (Proust et al., 2018), soybean (Wong et al., 2014; Bao et al., 2018), poplar (Su et al., 2018), cotton (Gu et al., 2014), common bean (Sosa-Valencia et al., 2017), and barley (Liu et al., 2014), and even in animals (Liu et al., 2018). STTMs have been introduced into plant cells through stable transformation (Yan et al., 2012), *Agrobacterium*-mediated transient expression (Zhang et al., 2017b), and virus-induced-gene silencing (Sha et al., 2014; Jian et al., 2017).

Whereas the design of plant TMs is based on the partial complementarity between miR399 and *IPS1*, there is higher complementarity between miRNAs and the artificial miRNA binding sites in STTMs and SPs. This allows STTMs/SPs to bind to the miRNAs more tightly and specifically. While SPs contain up to 15 miRNA binding sites linked by 4 nt of untested spacers, STTMs contain only one pair of miRNA binding motifs linked by an experimentally tested spacer of 48–88 nt that forms a weak ''stem-loop'' structure, leading to better stability of the STTM structures. Construction of multiple copies of identical miRNA binding sites poses a challenge to the application of SP technology, and all these miRNA sequestering techniques show variable efficacy in silencing different miRNAs (Reichel et al., 2015).

In this study, we applied STTM technology for a large-scale study of miRNA functions in *Arabidopsis thaliana* and the major crops rice, maize, and tomato. and generated hundreds of STTM constructs and a pool of transgenic plants as community resources for functional studies of miRNAs. We targeted individual miRNA families and simultaneously targeted two different miRNA families with distinct functions to delineate their interactive roles. Furthermore, we performed small RNA and RNA sequencing (RNA-seq) of STTM plants, which was effective in revealing new functions of miRNAs and their functional interactions. Importantly, we applied STTM in an inducible or tissue-specific manner, making it possible to study miRNA functions spatiotemporally and to improve grain yield without affecting plant growth and development. Finally, we created an online Genome Browser for the display of miRNA regulatory networks as revealed by RNA-seq and small RNA-seq of STTM transgenic plants.

RESULTS

Design of Constitutive, Inducible, and Tissue-Specific STTMs in Plants

STTM is a key technology for studying the effect of functional loss of a multi-membered miRNA family. To dissect miRNA functions, we designed and constructed hundreds of STTM constructs driven by the enhanced *35S* promoter to target highly conserved miRNA families as well as species-specific miRNAs (Figure 1A). These STTM constructs have been deposited in Addgene (Deposits 73 408 and 73 411, Supplemental Table 1).

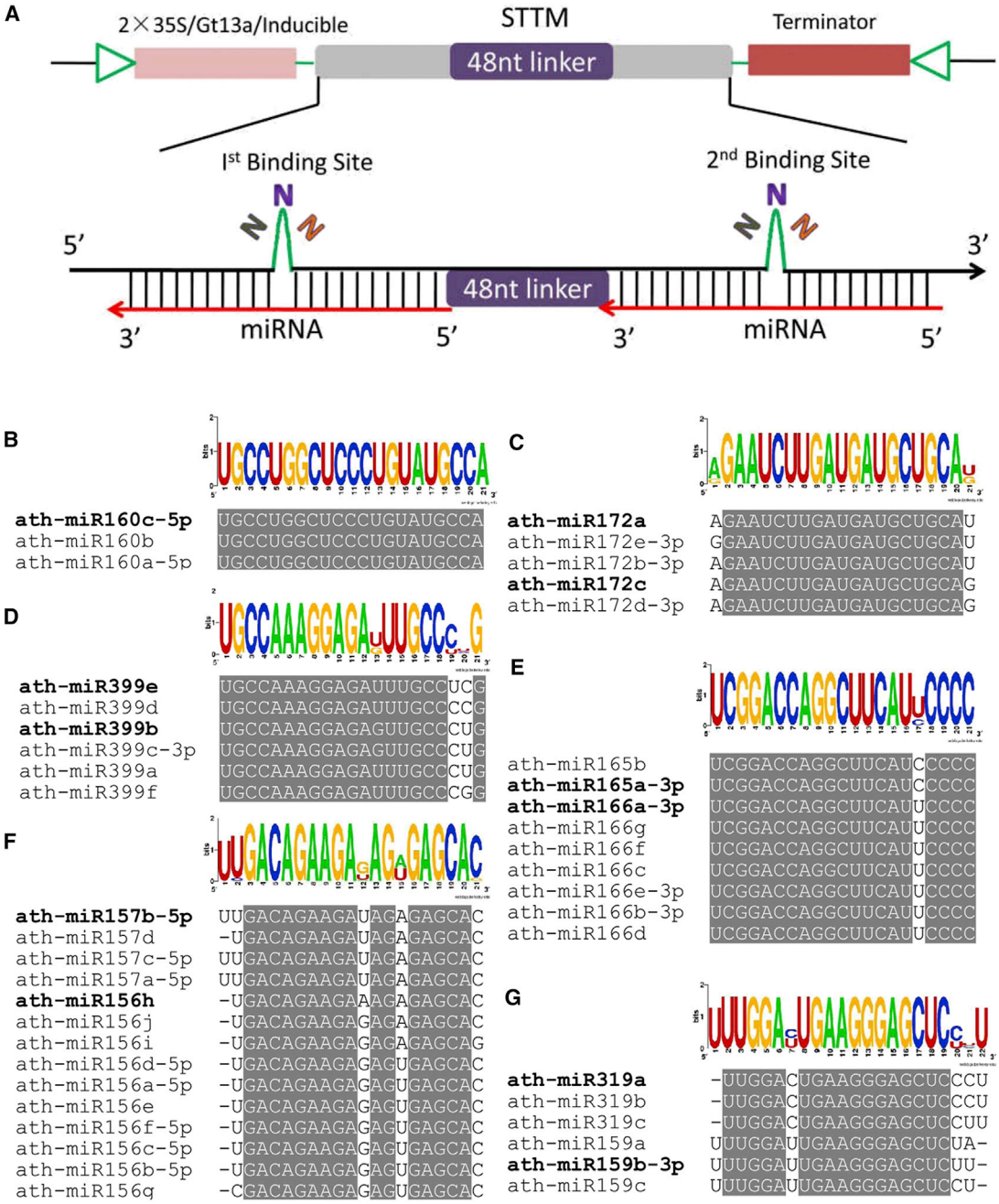

Figure 1. Diagrammatic Representation of an STTM Construct and Examples of Different miRNA Binding Sites Selected for Various STTM Constructs.

(A) Diagram showing the structure of the STTM with a 48-nt spacer and two non-cleavable miRNA binding sites. The enhanced *35S* promoter was used for constitutively expressing STTMs in *Arabidopsis*, tomato, rice, and maize; the β-estradiol inducible promoter was used for generating inducible STTM (iSTTM) lines, and the endosperm-specific Gt13a promoter was used for expressing STTMs targeting miRNAs in rice seeds.

(B–G) Examples of target miRNAs selected for designing the non-cleavable miRNA binding sites in STTMs. The degree of nucleotide conservation of the miRNAs in each group is indicated by the height of the letters (measured as bits). The nucleotides outlined by the white (variable) and gray (identical) boxes represent varied and conserved miRNA residues, respectively. The miRNA names marked in bold are the representative miRNA family members selected for designing non-cleavable miRNA binding sites.

The design of miRNA binding sites in STTM constructs was based on sequence comparisons of miRNA families and family members from different plant species. Specifically, two major members of an miRNA family or members of two different miRNA families, either evolutionarily conserved or species specific, were targeted by two non-cleavable miRNA binding sites with a 3-nt bulge between the 10th and 11th nucleotides, linked by a 48-nt spacer (Figure 1A). The two non-cleavable miRNA binding sites were designed for different situations as follows: (1) when the members of an miRNA family shared identical mature miRNA

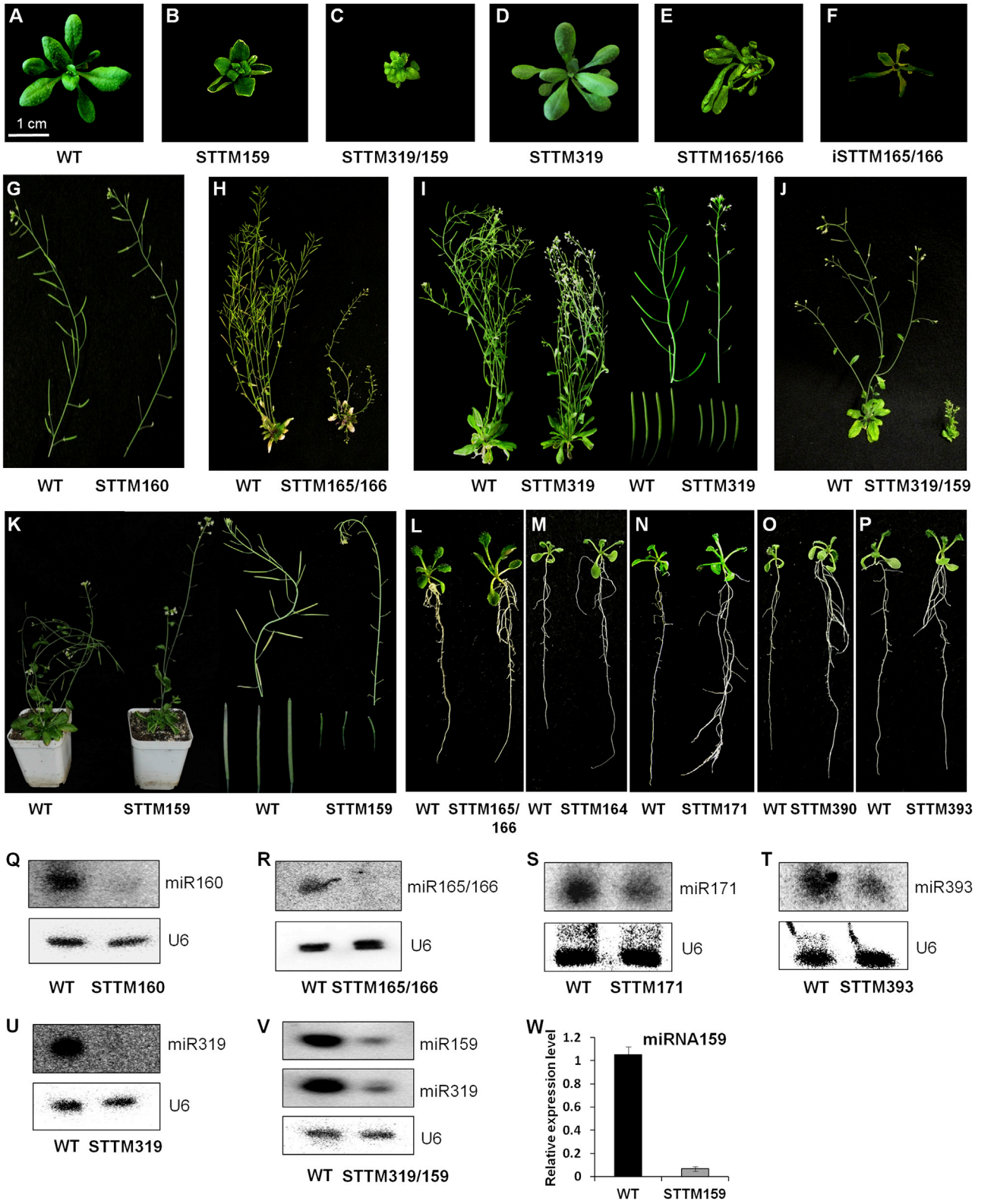

Figure 2. Phenotypes of Transgenic *Arabidopsis* Lines Expressing STTMs Targeting Various miRNAs.

(A–F) Three-week-old plants. **(A)** Wild-type (WT), **(B–E)** STTM159, STTM319/159, STTM319, and STTM165/166, respectively, driven by the enhanced *35S* promoter; **(F)** iSTTM165/166 driven by the inducible β-estradiol promoter. Scale Bar represents 1 cm for all panels.

(G–K) Partial sterility of STTM160 compared with WT shown at a later stage of fruit development **(G)**. The phenotypes of representative wild-type (WT) and STTM165/166 transgenic plants **(H)** at a later stage of fruit development. **(I)** The phenotypes of representative WT and STTM319 transgenic plants,

(legend continued on next page)

sequences, the same mature miRNA sequence was targeted by both tandem miRNA binding sites (Figure 1B); (2) when the members of an miRNA family had varied sequences, the sequences of two major variants were targeted separately by the tandem miRNA binding sites (Figure 1C and 1D); (3) two different miRNA families with distinct or partially conserved mature miRNA sequences were each targeted by one of the two miRNA binding sites in the same construct (Figure 1E–1G). For inducible STTM (iSTTM), we replaced the enhanced *35S* promoter with a β-estradiol-inducible promoter (Figure 1A). For seed-specific STTMs, we replaced the enhanced *35S* promoter with the endosperm-specific promoter Gt13a (Figure 1A).

Multiple Developmental Phenotypes Observed in *Arabidopsis* STTM Transgenic Lines

To test the effectiveness of the hundreds of STTMs that were generated, we subjected *A. thaliana* to large-scale transformation with STTMs, and scored the impact of STTMs on leaf development, root development, stature, and flowering. By observing different STTM transgenic lines in which different miRNAs were targeted, we found that miR156/157, miR160, miR165/166, miR167, miR171, miR319, miR159, and miR319/159 were involved in the development of leaf shape, as previously reported for some miRNAs (Allen et al., 2007; Todesco et al., 2010; Liu et al., 2011; Schommer et al., 2012; Yan et al., 2012; Yang et al., 2018) (Figure 2A–2F and Supplemental Figure 1). STTM159 transgenic plants were smaller than wild-type (WT) plants and had upward curled leaves (Figure 2B and Teotia and Tang, 2017). STTM319 transgenic lines had leaves with rounder apexes and shorter petioles compared with WT (Figure 2D). STTM319/159 transgenic plants had small rosettes and upward curled leaves (Figure 2C). STTM165/166 transgenic lines lost adaxial–abaxial polarity and had trumpet-shaped or upward-curling leaves and twisted stems (Figure 2E). Similar phenotypes were observed in inducible STTM165/166 transgenic lines, grown on half-strength Murashige and Skoog (MS) medium supplemented with 3 μM β-estradiol (Figure 2F and Supplemental Figure 2).

To evaluate the impact of knockdown of miRNA expression on reproductive development, we specifically examined the development of the siliques, seeds and seedset in the STTM transgenic plants. Of the lines in our *Arabidopsis* STTM transgenic collection, STTM159, STTM160, STTM165/166, STTM319, and STTM319/159 showed reduced seed set, as exemplified by the smaller numbers and sizes of siliques, as compared with the control (Figure 2G–2K). The overall plant stature and architecture were altered to different extents in these STTM plants. In addition, STTM160 and STTM165/166 had a semi-sterile phenotype, which further gave rise to reduced seed set (Figure 2G and 2H). Most seeds of STTM167 plants were noticeably underdeveloped, and the germination rate of STTM167 seeds was dramatically reduced (Supplemental Figure 3). For both STTM319 and STTM159, defects in seed development were apparent inside nearly all examined siliques (Figure 2I and 2K), while STTM319/159 was completely sterile (Figure 2J).

We then focused on those lines with STTMs targeting miRNAs related to auxin homeostasis and signal transduction, such as miR160, miR164, miR165/166, miR167, miR390, and miR393. We examined these STTM lines for changes in root development. The STTM164, STTM165/166, STTM171, STTM390, and STTM393 transgenic lines showed enhanced lateral root development, making the whole root system more robust than that of the control plant (Figure 2L–2P and Supplemental Figure 4). In contrast to the functions of the above auxin-related miRNAs in root development, loss of miR160 and miR167, both of which target auxin response factor genes, resulted in reduced seed set and germination, respectively (Figure 2G and Supplemental Figure 3).

Finally, we examined the flowering time of the STTM lines. The knockdown of miRNAs in STTM156/157, STTM172, and STTM160 led to early flowering (Supplemental Figure 5). In contrast, loss of miR167 delayed flowering as shown by about 15 rosette leaves compared with the control plants (Supplemental Figure 5C and 5F). Similar to our previous report (Yan et al., 2012), STTM triggered the degradation of miRNAs as shown by northern blots and/or qRT–PCR (Figure 2Q–2W and Supplemental Figure 6).

Important miRNA-Regulated Gene Networks Revealed by Small RNA-Seq and RNA-Seq of STTM Plants

To elucidate the molecular mechanisms underlying the phenotypes induced by STTMs, we selected and analyzed STTM156/157, STTM165/166, and STTM172 in detail by performing small RNA-seq and RNA-seq. From small RNA-seq analysis, we observed that reduction in the expression of these three miRNAs in STTM lines significantly altered other miRNA expression profiles (Figure 3 and Supplemental Tables 2–4). These results indicate that individual miRNAs crosstalk with many other miRNAs and that this contributes to the complex phenotypes of STTM156/157, STTM165/166, and STTM172 plants.

To further analyze the molecular functions of these three miRNAs at the transcriptome level, we constructed the overall gene ontology (GO) biological process enrichment profiles based on differentially expressed genes (DEGs) in the three STTM lines, STTM156/157, STTM172, and STTM165/166 (Supplemental Tables 5–7 and Supplemental Figure 7). Each STTM line showed distinct alterations in the expression of genes associated with various GO terms. All three STTM lines showed variation in gene expression related to anthocyanin biosynthesis and responses to various stimuli (Supplemental Figure 7). To validate the regulation of specific pathways by these miRNAs, we analyzed in detail the expression of genes involved in photosynthesis and anthocyanin biosynthetic pathways in STTM156/157 and abscisic acid (ABA) and auxin biosynthesis & signaling in STTM165/166 (Figures 4 and 5; Supplemental Figures 8–11). The phenotypes observed in

inflorescences, and siliques at a later stage of fruit development. **(J)** The phenotypes of representative WT and STTM319/159 transgenic plants. **(K)** The phenotypes of representative WT and STTM159 transgenic plants, inflorescences, and siliques at a later stage of fruit development.
(L–P) Two-week-old wild-type (WT), STTM165/166, STTM164, STTM171, STTM390, and STTM393 *Arabidopsis* seedlings.
(Q–W) Expression levels of the targeted miRNAs in the various STTM transgenic lines detected by northern blot analysis (**Q–V**) and stem-loop qRT–PCR **(W)**.

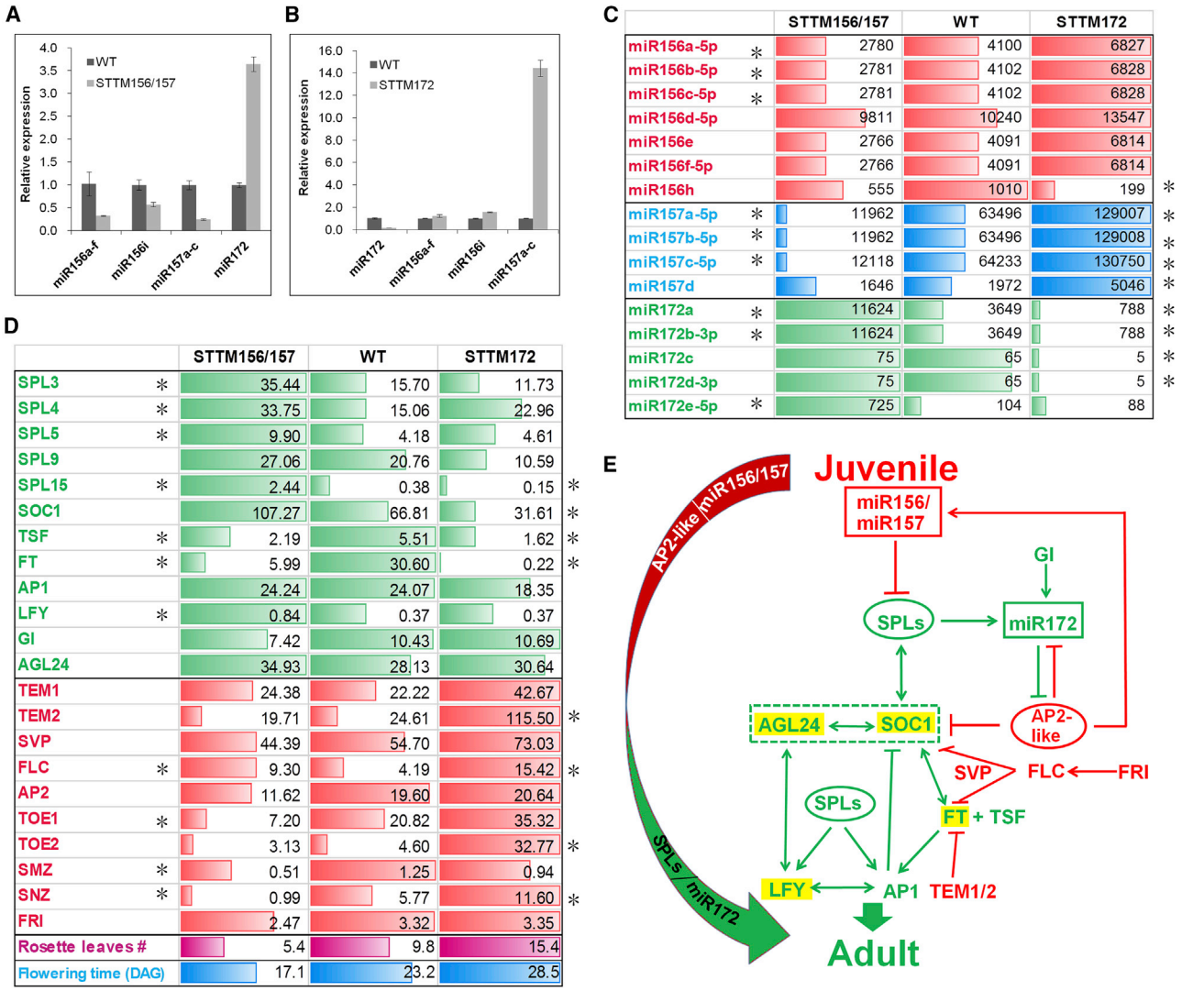

Figure 3. Expression Patterns of miR156/157, miR172, and Flowering-Time Genes Revealed by STTMs.

(A and B) The expression levels of miR156, miR157, and miR172 in STTM156/157 **(A)** and STTM172 **(B)** transgenic lines determined by qRT–PCR.

(C) The expression levels of miR156/157 and miR172 in STTM156/157 and STTM172 transgenic lines and WT determined by small RNA-seq. The numbers in the table are the normalized expression levels of the miRNAs, while the bars in the same row of the table indicates the relative expression of the same miRNA in STTM156/157, WT, and STTM172 transgenic lines. DEGs are marked with an asterisk.

(D) The expression levels of genes encoding flowering suppressors (in red) and activators (in green) in STTM156/157, WT and STM172 determined by RNA-seq. The bars in each row indicate the expression levels of the gene listed on the left. STTM156/157 plants flower early and show higher expression of flowering activators and lower expression of flowering repressors as compared with the WT, while the opposite trend is seen in late-flowering STTM172 plants. The second to last row (in purple) indicates rosette leaf numbers at the time of flowering and the bottom-most row (in blue) indicates flowering time in days after germination (DAG). DEGs are marked with an asterisk.

(E) A schematic of the flowering time pathway depicting various floral activators (in green) and repressors (in red) involved in regulating flowering time in *Arabidopsis*. Flowering integrators, FT, LFY, SOC1, and AGL24, are highlighted in yellow. *AGL24*, *AGAMOUS-LIKE 24*; *AP1/2*, *APETALA1/2*; *FLC*, *FLOWERING LOCUS C*; *FRI*, *FRIGIDA*; *FT*, *FLOWERING LOCUS T*; *GI*, *GIGANTEA*; *LFY*, *LEAFY*; *SMZ*, *SCHLAFMÜTZE*; *SNZ*, *SCHNARCHZAPFEN*; *SOC1*, *SUPPRESSOR OF CONSTANS1*; *SPL*, *SQUAMOSA PROMOTER-BINDING PROTEIN-LIKE*; *SVP*, *SHORT VEGETATIVE PHASE*; *TEM1/2*, *TEMPRANILLO1/2*; *TOE1-3*, *TARGET OF EAT1-3*; *TSF*, *TWIN SISTER OF FT*.

STTM156/157 and STTM165/166 were well explained by the results of these studies.

STTMs Altered the Expression of Target miRNAs and Underlying Networks Associated with Flowering Time

MiR156/157 and miR172 are two well-characterized miRNAs controlling flowering and the vegetative-to-reproductive transition in plants (Wu et al., 2009; Teotia and Tang, 2015). Loss of function of miR156/157 and miR172 in STTM lines induced early and late flowering, respectively (Supplemental Figure 5A and 5D). To understand how these two miRNAs regulate each other to regulate plant flowering, we performed deep sequencing to examine the changes in expression of miRNAs and flowering-related genes in the STTM156/157 and STTM172 transgenic lines and in WT plants, specifically at the flowering stage.

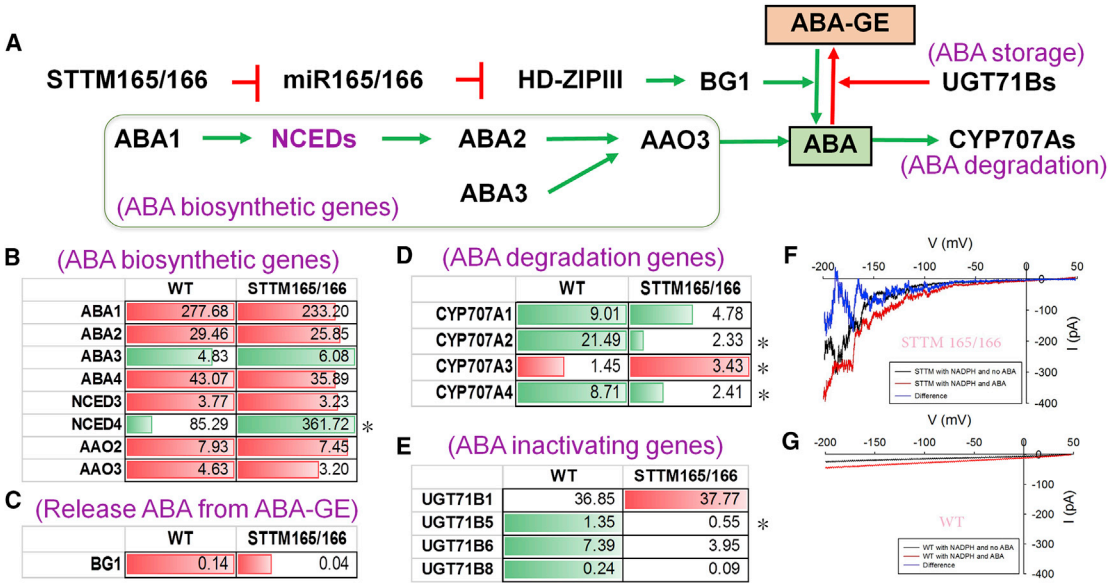

Figure 4. Enhanced Expression of ABA Biosynthetic Pathway Genes Resulted in ABA Accumulation in STTM165/166 Transgenic Lines.

(A) The ABA biosynthesis and metabolism pathway in *Arabidopsis*. ABA biosynthesis starts from violaxanthin, which through various steps is converted into abscisic aldehyde, which is oxidized into ABA by an abscisic aldehyde oxidase (AAO3). An additional biosynthetic pathway involves hydrolysis of Glc-conjugated ABA (ABA-GE) to ABA by two glucosidases. One glucosidase, BG1, is negatively and directly regulated by HD-ZIP III family transcriptional factors, which are targets of miR165/166. CYP707A family genes encode proteins with ABA 8′-hydroxylase activity. ABA uridine diphosphate glucosyltransferases (UGTs), UGT71Bs, convert active ABA to inactive ABA-GE.

(B–E) The expression levels of genes involved in ABA biosynthesis and metabolism. The bars in each row indicate the expression levels of the gene listed on the left, while green and red colors indicate whether the expression levels of the genes are consistent with or opposite to the phenotype of the STTM165/166 transgenic lines, respectively. DEGs are marked with an asterisk.

(F and G) ABA-activated Ca^{2+}-permeable currents were enhanced in STTM165/166 guard cell protoplasts. A large current was recorded in an STTM165/166 guard cell protoplast when there was only NADPH in the pipette solution, suggesting the pre-existence of ABA inside the cells. Addition of 50 μM ABA to the bath solution resulted in limited enhancement of the current **(F)**, suggesting that additional exogenous ABA did not trigger further Ca^{2+}-permeable currents. A small current was recorded in a WT guard cell protoplast when only NADPH was present, and addition of 50 μM ABA enhanced the current **(G)**.

Sequencing analysis showed that loss of either miR156/157 or miR172 led to alterations in the expression of other miRNAs (Supplemental Tables 2 and 4). Specifically, in the STTM156/157 transgenic lines, while the expression of miR156 and miR157 was reduced, the expression of miR172 was dramatically increased. In contrast, the STTM172 transgenic lines showed reduced expression of miR172 and increased expression of miR156 and miR157. Notably, loss of miR172 significantly increased the levels of miR157 but only slightly affected miR156 expression (Figure 3C, Supplemental Table 4). This finding was further validated by stem-loop qRT–PCR (Figure 3A and 3B). Whether and how miR157 and miR156 play different roles in modulating miR156/172-regulated flowering time and vegetative-to-reproductive phase change, needs to be further investigated by obtaining their respective knockout mutants through more effective approaches such as CRISPR/Cas9.

Analysis of the STTM156/157 and STTM172 lines also revealed the alteration of small RNA-regulated networks. The STTM156/157 transgenic lines showed increased levels of miR164c, miR169, and miR160c-3p and decreased expression of miR159a, miR160a,c-5p, miR160b, miR171, miR319a-c, miR408-3p, miR8175, and miR869.2, as compared with the control (Supplemental Table 2). Similarly, the STTM172 transgenic lines showed upregulation of miR160c-3p, miR164c-5p, and miR8183 and downregulation of miR156h, miR160a,c-5p, miR160b, miR163, miR319a-c, miR396-5p, miR408-3p, miR8175, and miR869.2 (Supplemental Table 4). Intriguingly, in STTM156/157 and STTM172 plants miR160c-3p was commonly up-regulated while miR160a, miR160c-5p, miR160b, miR319a-c, miR408-3p, miR8175, and miR869.2 were commonly down-regulated. Interestingly, miR169 was significantly upregulated in STTM156/157, but its expression was not affected in STTM172. Induction of miR169 under stress conditions triggers early flowering in *Arabidopsis* (Xu et al., 2014), and the up-regulation of miR169 could further contribute to the early-flowering phenotype of STTM156/157. In contrast, miR393 and miR171, which positively regulate flowering (Chen et al., 2011), were downregulated in STTM156/157. Furthermore, loss of function of miR160 (Supplemental Figure 5B) and miR319 (Sarvepalli and Nath, 2011) results in early flowering, which is consistent with the low expression of these miRNAs in early-flowering STTM156/157 plants, but does not explain their low expression levels in STTM172 plants, which has a late-flowering phenotype.

Altered expression of miR156/157 and miR172 in STTM lines also changed the expression of flowering genes (Figure 3D; Supplemental Tables 5 and 7). We found about 40 and 65 differentially expressed flowering genes in STTM156 and STTM172, respectively, compared with WT (Supplemental Table 8). The flowering genes database (http://www.flor-id.org) provides a reference for flowering genes (Bouche et al., 2016).

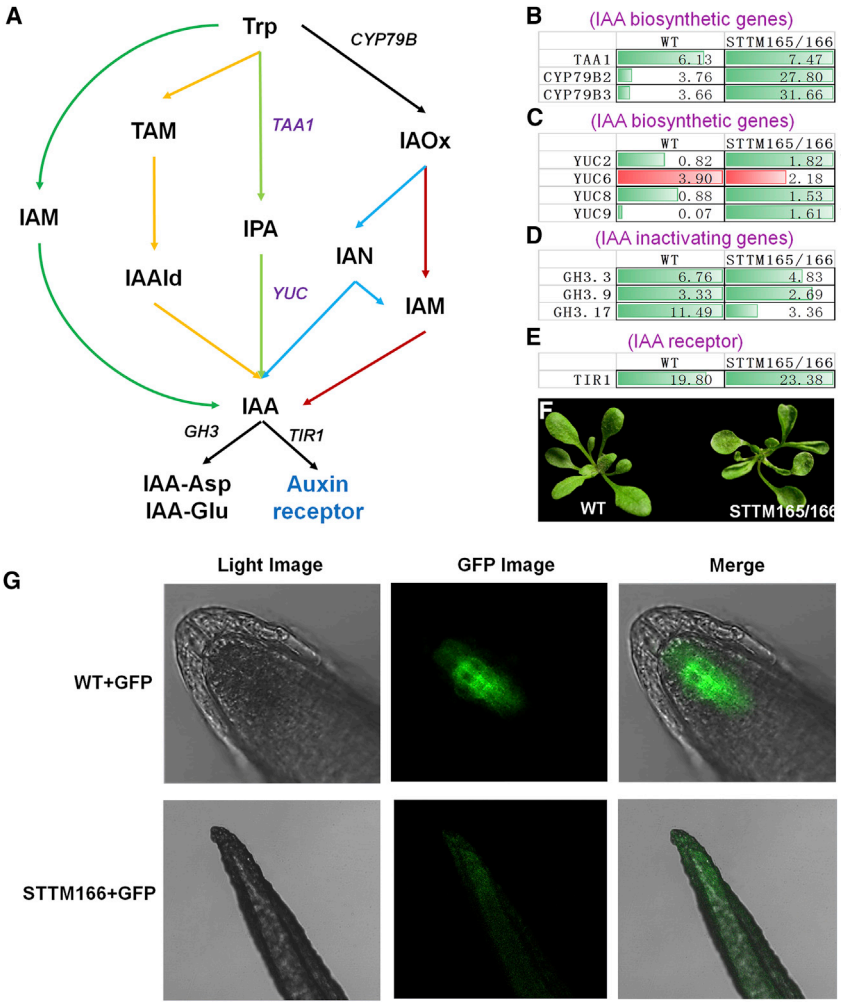

Figure 5. Upregulation of Indole-3-acetic acid (IAA) Biosynthesis and Metabolism Pathway Genes in STTM165/166 *Arabidopsis* Transgenic Lines.

(A) The IAA biosynthesis and metabolism pathways in *Arabidopsis*. There are four proposed pathways for the biosynthesis of IAA from tryptophan in *Arabidopsis* (Mashiguchi et al., 2011): (1) the indole-3-pyruvic acid (IPA)–YUCCA (YUC) pathway, (2) the tryptamine (TAM) pathway, (3) the indole-3-acetamide (IAM) pathway, and (4) the indole-3-acetaldoxime (IAOx) pathway. Inactive IAA-Asp and IAA-Glu are biosynthesized from active IAA by GH3 family enzymes. TIR1 is the auxin receptor in *Arabidopsis*. The purple and red arrows indicate the up- and downregulation of genes in the pathway, respectively.

(B–E) The expression levels of genes involved in IAA biosynthesis and metabolism. The bars in each row indicate the expression levels of the gene listed on the left, and the green and red colors indicate whether the expression levels of the genes are consistent with or opposite to the phenotype of the STTM165/166 transgenic lines, respectively. DEGs are marked with an asterisk.

(F) Higher levels of auxin induced the development of upward tilted, spoon-shaped cotyledons and abnormal rosette leaves in a 2-week-old STTM165/166 transgenic plant.

(G) *DR5rev*::*GFP* expression in STTM165/166 and WT. The usual auxin maxima was missing at the root apex, and the auxin gradient was more diffuse in STTM165/166 plants.

At the flowering stage, almost all of the flowering activators and repressors listed in this database were up- and downregulated, respectively, in STTM156/157 plants compared with WT. Opposite expression patterns for these genes were observed in STTM172 flowering plants (Figure 3D, Supplemental Tables 5, 7, and 8). The expression levels of most flowering activators and repressors, except the three flowering integrators (*FT*, *LFY*, and *AGL24*), were fully consistent with the flowering times of the STTM lines and were in general agreement with flowering pathway regulation (Figure 3D and 3E; Supplemental Tables 5, 7, and 8). Intriguingly, STTM156/157 lines showed early flowering and had a lower level of FT expression compared with WT (Figure 3D and Supplemental Table 8). This apparent contradiction may be due to the fact that flowering is a complex phenomenon wherein many pathways crosstalk with each other. If some positive flowering regulators such as *FT* are downregulated in STTM156, this indicates that some other positive factors may be upregulated or that negative regulators are downregulated, still shifting the overall commitment toward early flowering. Consistent with the phenotypes of STTM156/157, *35S*::*MIM156* plants also flowered early and *FT* expression was slightly down-regulated at the 8-day stage (Kim et al., 2012). Here, the lower expression of *FT* may be caused by the higher expression of *FLC*, a repressor of *FT* (Figure 3D and 3E; Supplemental Table 8), while other factors could compensate for the negation of *FT* activity, eventually leading to early flowering. Thus, FT expression dynamics and its relationship with other flowering regulators requires further investigation.

RNA-Seq Analysis of STTM156/157 Revealed Roles of miRNA156/157 in Anthocyanin Biosynthesis and Photosynthesis

To study the regulatory networks of miR156/157 in *Arabidopsis*, we performed RNA-seq analysis of STTM156/157. First, we found that the well-recognized miR156/157 target genes, SPLs, were upregulated (Figure 3D), suggesting that the STTM156/157 lines were indeed miR156/157 knockdown lines. The upregulation of various flowering-time and floral identity regulators including miRNAs, such as miR172, and genes, such as *SOC1*, *LFY*, *FUL*, *AGAMOUS-LIKE 42* (*AGL42*), and other MADS box genes, provides further evidence that we produced the correct STTM156/157 lines (Figure 3D and Supplemental Table 8). These genes are presumably upregulated by the miR156/157-targeted SPLs through binding to their promoters.

Next, we examined the RNA-seq data for STTM156/157 lines to identify new pathway genes potentially regulated by

miR156/157. Altogether, up to 2481 transcripts were differentially expressed in STTM156/157 transgenic plants, in comparison with the control plant (Supplemental Table 5). GO analysis of these DEGs in STTM156/157 revealed them to be enriched in pathways that are related to the generation of precursor metabolites and energy, anthocyanin-containing compound biosynthetic processes, and response to chitin, wounding, jasmonic acid, mechanical stimulus, and other functions (Supplemental Figures 7 and 8). In addition, the leaves of *Arabidopsis* STTM156/157 plants were darker green compared with those of control plants (Supplemental Figure 9F and 9G), suggesting a likely change in photosynthesis pathways. Indeed, almost all of the genes encoding photosystem I (PSI) and PSII component proteins, such as *PSBQ-2*, *PSBQA*, and *PSBO2* in PSII, and *PSAD-2*, *PSAF*, and *PSAH2* in PSI, were upregulated in STTM156/157 (Supplemental Figure 9A–9E and Supplemental Table 9). Consistent with this, DEGs between STTM156/157 and WT are also involved in starch and sucrose metabolism (Supplemental Figure 10). This indicates that miR156/157 may negatively regulate photosynthesis by altering the abundance of photosynthetic components including chlorophyll levels in *Arabidopsis*.

In addition, less anthocyanin accumulation in the stem was observed in STTM156/157 plants (Supplemental Figure 11C and 11D). Consistent with this observation, RNA-seq data revealed that genes involved in regulating flavonoid and anthocyanin biosynthesis were downregulated in STTM156/157 transgenic lines as compared with the control plant (Supplemental Figures 11A, 11B, 11E, 11F, and 12; Supplemental Tables 5 and 10).

Compared with STTM156/157, STTM172 plants showed similar expression patterns of anthocyanin and flavonoid biosynthesis genes (Supplemental Figures 13 and 14; Supplemental Table 10). Like STTM156/157, expression levels of most of the key anthocyanin biosynthesis genes were also lower in STTM172 compared with WT, but the expression levels of these genes were not as low as in STTM156 (Supplemental Tables 5, 7, and 10). In contrast, STTM165/166 showed more active phenylpropanoid biosynthesis than the other two STTM lines (Supplemental Figure 13). Flavonoids and anthocyanins are synthesized through the phenylpropanoid pathway in plants. This is consistent with GO enrichment of anthocyanin and flavonoid biosynthesis pathway genes in STTM165/166 (Supplemental Figures 7 and 8). Furthermore, STTM165/166 plants accumulated significantly more anthocyanin than WT plants (Supplemental Figure 15). Like STTM156, STTM172 also showed higher expression levels of most photosynthesis-related genes compared with WT (Supplemental Tables 5, 7, and 9). Thus, with respect to anthocyanin and flavonoid biosynthesis and photosynthesis, miR156 and miR172 share similar functions.

STTM165/166 Reveals the Involvement of miR165/166 in ABA and Auxin Biosynthesis and Signaling

STTM165/166 induced the knockdown of miR165/166 in *Arabidopsis*. DEGs in STTM165/166 determined by RNA-seq were enriched in pathways related to the generation of precursor metabolites and energy, anthocyanin-containing compound biosynthetic processes, and, of particular interest, response to ABA and auxin signaling (Figures 4 and 5; Supplemental Figures 7 and 16). By examining the pathway genes related to ABA and auxin signaling, we found that the gene encoding the rate-limiting enzyme in ABA biosynthesis 9-*cis*-epoxycarotenoid dioxygenase (*NCED4*) (Tan et al., 1997; Taylor et al., 2000) was significantly upregulated in STTM165/166. Interestingly, most *CYP707A* family genes encoding ABA 8′-hydroxylase proteins were downregulated. In contrast, genes involved in the conversion of ABA to the inactive ABA-glucose ester (ABA-GE), such as *UGT71Bs*, were downregulated in STTM165/166 (Figure 4A–4E). Furthermore, in STTM165/166 plants a strong ABA-activated calcium current was recorded compared with WT, which may have been induced by high endogenous ABA levels in the STTM mutant (Figure 4F and 4G). Taken together, loss of miR165/166 in *Arabidopsis* altered gene expression related to ABA biosynthesis and signaling (Figure 4).

Further analysis of the RNA-seq data for STTM165/166 revealed that the expression of genes in the auxin biosynthesis pathway also changed. Specifically, genes in the indole-3-pyruvic acid (IPA)–YUCCA (YUC) pathway were significantly upregulated. *CYP79B* family genes in the indole-3-acetaldoxime (IAOx) pathway and *TIR1* (an auxin receptor) were also upregulated. In contrast, *GH3* family genes, which encode enzymes that promote the formation of inactive IAA-Asp and IAA-Glu, were downregulated. Taken together, loss of miR165/166 promoted the production of active auxin (Figure 5A–5F). Analysis of *DR5rev*::*GFP* (Friml et al., 2003) expression in STTM165/166 roots showed that the usual auxin maxima was missing at the root apex and that the auxin gradient was more diffused, indicating abnormal auxin distribution in STTM165/166 plants (Figure 5G). This could be related to abnormal auxin transport.

Tissue-Specific STTM Expression Is a Powerful Way to Manipulate Rice Grain Size without Affecting Normal Plant Development

While expression of STTM159 in rice under the control of the enhanced *35S* promoter led to smaller seed grains and plants (Zhao et al., 2017; Gao et al., 2018), tissue-specific knockdown of miRNAs led to an increase in seed size (Figure 6A–6D; Zhao et al., 2018). To apply STTM technology for crop improvement while avoiding adverse impacts on normal plant development, we used the endosperm-specific promoter Gt13a to downregulate two grain-filling-related miRNAs (miR167 and miR1432) in rice. Rice plants with STTM167 and STTM1432 expression driven by Gt13a, developed normally but produced larger grains (Figure 6A and 6B). In 35S-STTM159 transgenic rice the grain weight decreased by 33.66% compared with the control, whereas in Gt13a-STTM167 and Gt13a-STTM1432 it increased by 26.31% and 15.21%, respectively (Figure 6E). More specifically, in 35S-STTM159 grain length, width, and thickness decreased by 18.53%, 7.62%, and 8.86%, respectively (Figure 6F–6H). In Gt13a-STTM167 and Gt13a-STTM1432 grain length increased by 6.94% and 7.57% (Figure 6F), and grain width increased by 6.46% and 3.87% (Figure 6G), respectively. In addition, in Gt13a-STTM167 plants grain thickness increased by 2.96% (Figure 6H). Taken together, these results suggest that application of STTMs in a tissue-specific manner could allow the modulation of grain production in rice, making it a powerful tool for crop improvement.

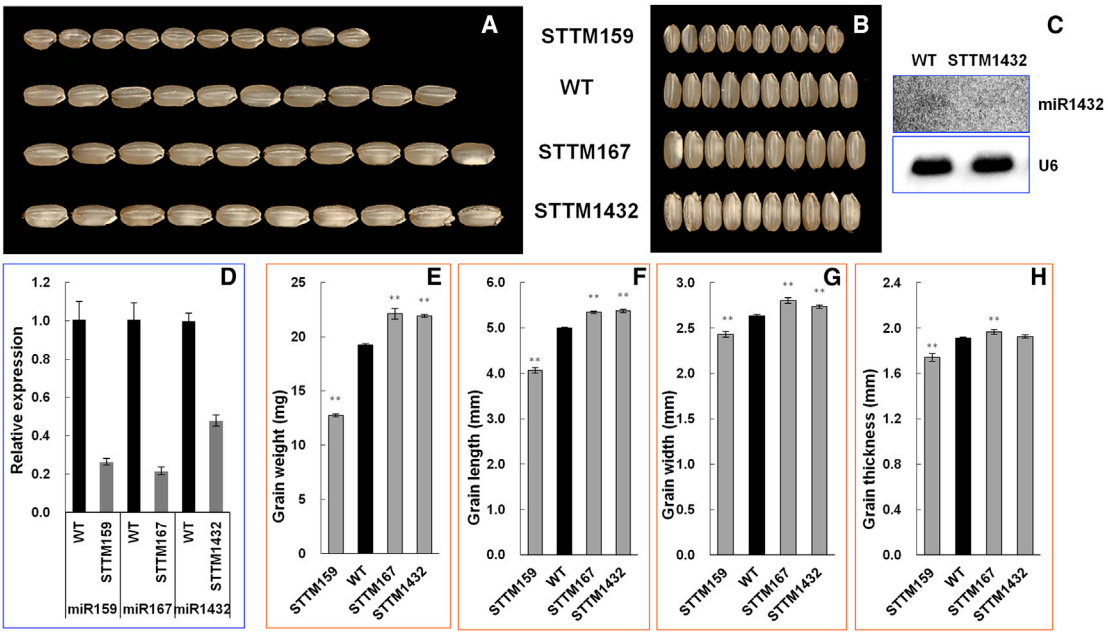

Figure 6. Seed-Specific Expression of STTMs Enhanced Productivity in Rice.

(A) Rows of 10 seeds from enhanced 35S-STTM159, WT, Gt13a-STTM167, and Gt13a-STTM1432 plants, arranged to show the grain lengths.

(B) Rows of 10 seeds from enhanced 35S-STTM159, WT, Gt13a-STTM167, and Gt13a-STTM1432 plants, arranged to show the grain widths.

(C) The expression level of miR1432 in Gt13a-STTM1432 transgenic seeds determined by northern blotting.

(D) The expression levels of miR159, miR167, and miR1432 in transgenic seeds determined by qRT–PCR.

(E–H) Grain weight **(E)**, grain length **(F)**, grain width **(G)**, and grain thickness **(H)** for WT and STTM159, STTM167, and STTM1432 transgenic rice. In transgenic rice, expression of STTM159 was driven by the enhanced *35S* promoter, whereas the expression of STTM167 and STTM1432 was driven by the Gt13a endosperm-specific promoter. Asterisks indicate significant difference compared to WT plants.

STTMs Triggered the Loss of Function of Maize miRNAs with or without miRNA Degradation

In *Arabidopsis*, STTMs primarily trigger the degradation of the targeted miRNAs. To test the effectiveness of STTMs in the monocot maize, we constructed STTM166 and STTM172 and transformed them into maize. Transgenic STTM lines displayed the expected phenotypes. Maize STTM166 plants had a defect in leaf development primarily resulting in rolled leaves (Figure 7A). These STTM166 transgenic plants were further assayed for the expression of miR166 and, similar to what was observed in *Arabidopsis*, 95% of miR166 was degraded (Figure 7D and Supplemental Figure 17A). Tassel seed phenotypes similar to those of *ts4*, a mutant with loss of function of the miR172e gene (Chuck et al., 2008), were observed in nearly all STTM172 transgenic lines as expected (Figure 7B and 7C). In addition, the time from sowing to tasseling and to maturity was much longer for STTM172 maize transgenic lines than for WT control plants (Supplemental Figure 17C and 17D). Surprisingly, the expression levels of miR172 in these transgenic lines were almost identical to those in WT control plants (Figure 7E and Supplemental Figure 17B), suggesting that STTM172 induced functional loss rather than degradation of miR172 in maize.

STTMs Are Useful Tools for Manipulating miRNA Expression to Improve Productivity in Tomato

To explore the potential applications of STTM technology in modulating fruit development, we used STTMs to constitutively downregulate two well-conserved miRNAs, miR165/166 and miR396, in tomato (Figure 8). STTM165/166 tomato plants were of short stature and had curled and twisted leaves with abnormal phyllotaxy (Figure 8A and 8B). Remarkably, blocking the expression of miR396 resulted in a larger plant, with bigger flowers, leaves, and fruits (Figure 8C–8E and Supplemental Figure 18). In both STTM165/166 and STM396 transgenic lines, the expression levels of the targeted miRNAs decreased as confirmed by northern blotting (Figure 8F and 8G).

A Resource for the Distribution of STTM Constructs and an STTM JBrowser (STTMJB) for Displaying miRNA Regulatory Networks

To facilitate the use of the STTM collection generated in this study, we submitted hundreds of STTM constructs (Supplemental Table 1), for use in either monocot or dicot plants, to Addgene (http://www.addgene.org/Guiliang_Tang/). Phenotypic changes in these STTM transgenic lines are documented (Figures 2, 5, 6, 7, and 8; Supplemental Table 1). A web-based tool termed designSTTM has been developed to demonstrate how these STTMs were constructed (https://blossom.ffr.mtu.edu/). For each specific STTM, designSTTM automatically stores results into the database, and a sketch of a plasmid construct is plotted with all boundaries between different fragments and the lengths of all fragments being clearly labeled (Supplemental Figure 19). When a design process is completed, an annotated report detailing the steps of STTM construction is generated. Users can print the sketch of each plasmid vector together with the construction protocol.

To visualize the alteration in miRNA regulatory networks in response to the loss of miRNAs triggered by STTMs, we used

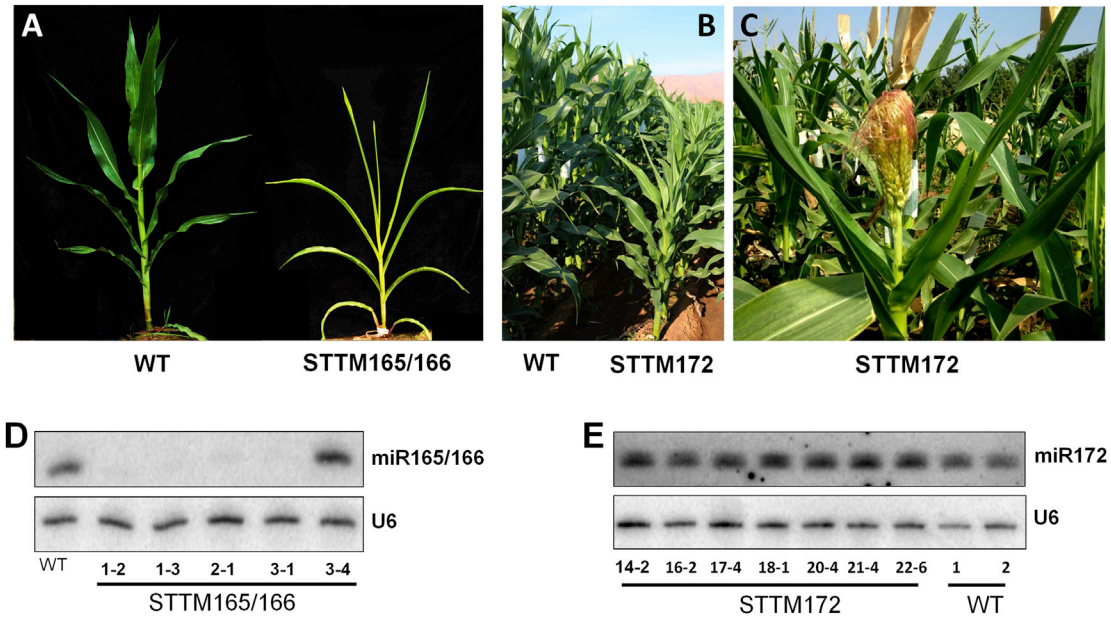

Figure 7. STTMs Induced miRNA Degradation (with or without Sequestering) in Maize.
(A) STTM166 plants showed rolled leaves.
(B and C) Phenotypes of a maize STTM172 transgenic plant **(C)** displaying tassel seeds and late flowering and a WT plant **(B)**.
(D) Expression levels of miR166 determined by northern blotting, showing the degradation of miR166 in the STTM166 line.
(E) Expression levels of miR172 in the STTM172 transgenic line determined by northern blotting showing that STTM172 did not trigger the degradation of miR172.

JBrowser (Skinner et al., 2009) to display the gene expression reads mapped to genes of interest from specific pathways in plants with a sequenced genome. This browser, STTMJB, accepts and displays RNA-seq and small RNA-seq data for STTM transgenic plants and their controls (https://blossom.ffr.mtu.edu/designindex2.php). As an example, we have displayed the DEGs related to major physiological processes such as anthocyanin biosynthesis in *Arabidopsis* STTM156/157 (Supplemental Figure 12).

DISCUSSION

STTMs Are Valuable Tools for Dominant Knockdown of miRNAs in Plants

STTMs can induce loss of functions in miRNAs that can be observed in both homo- and heterozygotes, making it possible to study the functions of miRNAs at a very early stage in a relatively simple background. Not all STTM transgenic plants showed apparent morphological changes. However, the reduction in the expression levels of miRNAs and upregulation of their target genes could be detected by northern blots and qRT–PCR. This suggests that not all miRNAs have critical roles in plant growth and development. Some of them may regulate metabolic processes that may not result in any developmental phenotypes when disrupted. Phenotypes for plants with knockdown of stress-related miRNAs, may only be apparent under stress conditions. For example, miR395 and miR399 are expressed at a low level in *Arabidopsis* under normal conditions but are induced by sulfur and phosphate starvation conditions, respectively (Fujii et al., 2005; Kawashima et al., 2009, 2011). It has also been shown that STTMs could simultaneously downregulate multiple unrelated miRNAs by using increased number of tandem repeats targeting different miRNAs (Fei et al., 2015). This allows STTMs to be used to knock down unrelated miRNAs, belonging to different families. Beyond miRNAs, STTMs have also been successfully used to silence the expression of siRNAs (McCue et al., 2013; Wang et al., 2018).

Approaches to Studying miRNA Functions Using the STTM Resource

Unlike in animals, in which a single miRNA can target and regulate hundreds of transcripts and a single transcript may be targeted by a number of miRNAs (Lewis et al., 2003), plant miRNA regulatory networks are much simpler, making it easier to study specific regulatory networks (Jones-Rhoades and Bartel, 2004; Rubio-Somoza and Weigel, 2011). With a defined STTM transgenic line, such as STTM156/157, in which miR156/157 is repressed and SPL family target genes are upregulated, one can look at the gene networks that are under the control of an miRNA family. These gene networks can be revealed by small RNA-seq (Figure 3C and Supplemental Tables 2–4) and RNA-seq (Figure 3D and Supplemental Tables 5–7). By using such an approach, we demonstrated that miR156/157 and miR172, which have opposite regulatory roles in flowering (Teotia and Tang, 2015), inversely regulate each other to modulate plant flowering time (Figure 3). SPL9 and SPL10 induce the expression of miR172b (Wu et al., 2009). Thus, induction of SPL9 and SPL10 expression in STTM156/157 can in turn lead to up-regulation of miR172. The inconsistent expression patterns of some miRNAs with respect to the flowering phenotypes of STTM156/157 and STTM172 indicates that miR156/157 and miR172 play predominant roles in

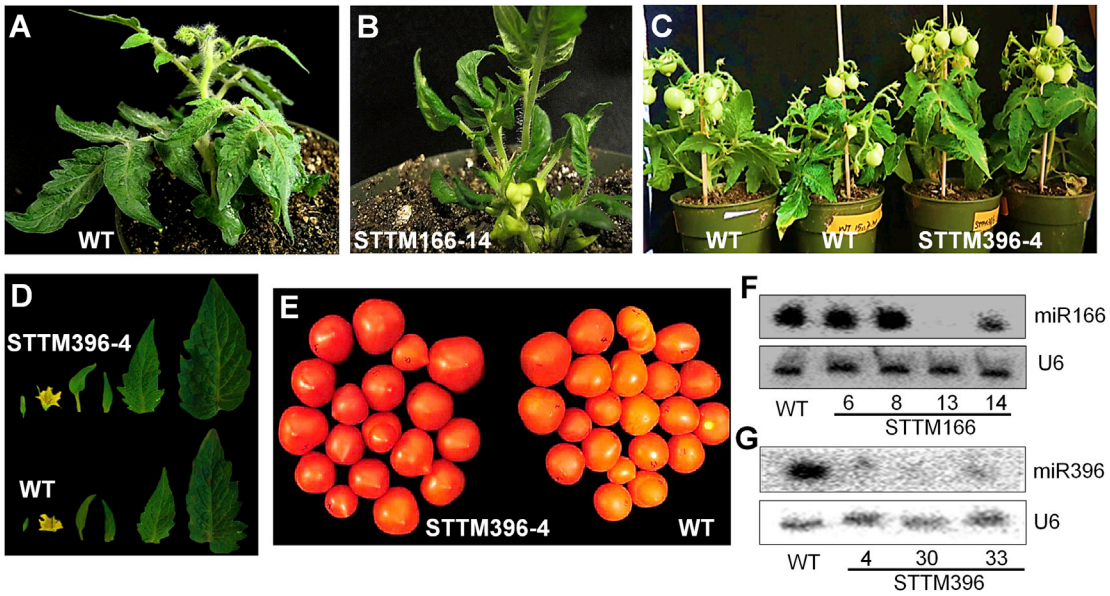

Figure 8. STTMs Affected Plant Development and Productivity in Tomato.

(A and B) Compared with the WT **(A)**, STTM165/166 transgenic tomato line #14 showed twisted leaves and abnormal phyllotaxy **(B)**.

(C–E) STTM396 transgenic tomato line #4 was taller than WT**(C)** and had bigger leaves **(D)** and bigger fruits **(E)**. For quantitative data, see Supplemental Figure 18.

(F and G) Northern blots showing the reduction in the levels of miR166 in STTM166 transgenic lines **(F)** and of miR396 in STTM396 transgenic lines **(G)** compared with the WT.

complex flowering programs, and somehow bypass other miRNAs with regulatory roles in flowering, such as miR160, miR393, and miR319. The differential expression levels of various floral activators and repressors in STTM156/157 and STTM172 plants reveal that miR156 and miR172 modulate the timing of flowering not only by interacting with each other but also by regulating the expression of many flowering time genes through regulation of their target genes. STTM156/157, STTM172, and WT flowered at different times and floral activators and repressors were expressed at different levels in these lines. A certain level of inconsistency in the expression patterns of some flowering integrators was observed in STTM156/157 and STTM172, compared with WT, suggesting that these flowering integrators were regulated differently in these plants. This differential expression of flowering genes was sufficient to promote early flowering in the case of STTM156/157, or delayed flowering in the case of STTM172.

Other important findings from the study of STTM lines are that miR156/157 regulate photosynthesis and anthocyanin biosynthesis and that miR165/166 regulate ABA and auxin biosynthesis and signaling, and also ABA-guided ion-channel activities in leaf cells. Some of these findings confirm previous observations, such as the role of miRNA156/157 in anthocyanin biosynthesis (Gou et al., 2011) and the roles of miR165/166 in auxin biosynthesis (Jia et al., 2015), and in drought and cold stress tolerance through alteration of ABA biosynthesis (Yan et al., 2016). Furthermore, the role of miR156/157 in enhancing photosynthesis (Supplemental Figure 9) was revealed by RNA-seq and informatics analyses of the STTM lines. PHABULOSA (a target of miR165/166) directly binds to and upregulates the expression of *BG1* and *ABI4* (Yan et al., 2016). *BG1* encodes a β-glucosidase, which releases free biologically active ABA from the inactive ABA-GE, and *ABI4* along with *ABI3* and *ABI5* regulates the expression of ABA-responsive genes. STTM165/166 plants showed no significant change in *BG1* and *ABI4* expression. This discrepancy may be due to the differences in the tissue developmental stage examined, which may affect the observation of tissue and gene expression responses to ABA. Further study is required to determine the mechanism underlying this observation.

miR165/166 targets control the expression of *LEC2*, which activates the expression of the *YUCCA* auxin biosynthesis genes. REVOLUTA, an miR165/166 target, directly binds to and increases the expression of auxin biosynthetic genes, *TAA1* and *YUC5* (Brandt et al., 2012). This could explain the higher auxin content in STTM165/166 compared with WT. By analyzing *DR5rev*::*GFP* expression, we showed that auxin is mislocalized in the root tips of STTM165/166 plants, indicating an auxin transport problem. Altered *DR5rev*::*GFP* distribution in STTM165/166 could be due to changes in PIN expression or localization, which needs to be further investigated.

miR156 has been shown to regulate chlorophyll biosynthesis and photosynthetic rate in tobacco. miR156 overexpressing plants have pale green leaves while plants with reduced expression of miR156 have dark green leaves (Feng et al., 2016). The cause of higher chlorophyll content in STTM156/157 plants and how miR156 is involved in chlorophyll biogenesis or degradation is still largely unknown. However, it has been shown that an *Arabidopsis* mutant (*ch1-4*) with impaired chlorophyll *a* oxygenase, which blocks the biosynthesis of chlorophyll *b*, accumulates more miR156, shows a delayed phase change, and a lower photosynthetic rate, indicating the negative feedback of chlorophyll content on miR156. Furthermore, sugar

produced by photosynthesis acts as a developmental cue for the juvenile-to-adult phase transition, whereby increased sugar levels suppress miR156 expression (Yang et al., 2013; Yu et al., 2013). We believe that STTM-induced repression of miR156 activates the SPLs, which accelerates the onset of the adult phase marked by activated biogenesis of chlorophyll, increased photosynthetic rate, and increased sugar accumulation. Our study confirms that miR156 regulates chlorophyll biosynthesis in *Arabidopsis*. The expression levels of anthocyanin biosynthetic genes, such as *DFR*, *ANS*, *F3′H*, and *UGT75C1*, were lower in plants with suppressed expression of miR156. Elevated levels of SPL9 in STTM156/157 plants likely suppress *DFR* expression by disrupting the MYB-bHLH-WD40 transcriptional-activation complex (Gou et al., 2011). Also, SPL9 competes with TT8 for binding to PAP1, which in turn regulates the expression of anthocyanin biosynthesis genes. As observed in STTM156/157, most of the key anthocyanin biosynthesis genes were downregulated and photosynthesis genes were upregulated in STTM172 compared with WT. We believe that the unknown regulatory networks of these two miRNAs control common downstream factors.

In summary, we have provided examples of the use of STTM technology to interrogate the functional networks of specific miRNAs. Similar approaches may be taken using the hundreds of STTM constructs that have been made available to the community. Moreover, with STTM technology one is able to study not only functions of a single miRNA (Yan et al., 2012) but also the interactions between two miRNAs. For example, to study the interaction between miR319 and miR159, we constructed and generated STTM319/159 transgenic lines (Figure 2C and 2J). These transgenic plants showed a decrease in the expression levels of both miR319 and miR159 (Figure 2V) and exhibited dwarfism, upward curled leaves, and sterile flowers. These phenotypes mimics those of a hybrid plant obtained by crossing MIM319 (partly fertile) and MIM159 (upward curled leaves and partly fertile) (Rubio-Somoza and Weigel, 2013). In another example, miR170 and miR171 were targeted by a single STTM, and both miR170 and miR171 were downregulated as shown by stem-loop qRT–PCR (Supplemental Figure 6). However, the STTM170/171 transgenic lines had no apparent phenotypes. Another potential approach for studying miRNA interactions is to cross two or more different STTM lines with each other. This will generate double or triple STTMs that downregulate two or more miRNAs, allowing their functional interactions to be investigated. Taken together, STTMs and STTM transgenic lines are valuable resources for the study of miRNA regulatory networks and miRNA interactions in plants.

STTM Can Be Used as a Tool for Improving the Grain and/or Fruit Yield in Crops

Many miRNAs function in the modulation of crop traits that enhance productivity (Zuo and Li, 2014). For example, miR156 expression increases during rice grain development and during other developmental stages (Peng et al., 2013, 2014). Three of its target genes, *SPL13*, *SPL14*, and *SPL16*, have been reported to be involved in regulating rice seed production-related traits, whereby *SPL14* negatively regulates tiller number and positively controls rice panicle and seed number per panicle (Jiao et al., 2010; Miura et al., 2010) and *SPL13* and *SPL16* promote rice seed size (Wang et al., 2012; Si et al., 2016). Thus the ideal plant architecture with larger seed size could be expected in STTM156 transgenic rice in which *SPL14* and *SPL16* are more highly expressed. Blocking miR396, or overexpressing its target gene, *GRF* (growth regulating factor), could increase fruit yield in tomato (Figure 8E and Supplemental Figure 18E) and promote panicle branching and grain weight in rice (Che et al., 2015; Duan et al., 2015; Gao et al., 2015; Cao et al., 2016; Li et al., 2016; Sun et al., 2016). STTM-mediated silencing of miR398 was found to decrease seed size in transgenic rice (Zhang et al., 2017a). In contrast, STTM-mediated silencing of miR5144-3p increased grain weight in transgenic rice (Xia et al., 2018). Additionally, higher expression of some miRNAs in rice, such as miR319 (Wang et al., 2014) and miR393 (Bian et al., 2012; Xia et al., 2012), decreased one or more seed production-related traits, including seed number, seed size, and tiller number. STTMs could be used to lower the expression levels of miRNAs with negative effects on seed traits in rice to establish a larger seed or panicle.

Given that miRNAs may affect multiple developmental processes, silencing of these miRNAs in a temporal and spatial manner, using inducible or tissue-specific promoters, is necessary to avoid pleiotropic effects without penalizing yield. Previous studies reported that the expression levels of a majority of miRNAs gradually increase during rice seed development (Zhu et al., 2008; Lan et al., 2012; Peng et al., 2013, 2014; Yi et al., 2013). These miRNAs may play important roles in determining seed production by regulating grain-filling. In this study, we blocked the expression of two of these miRNAs, miR167 and miR1432, using a seed-specific promoter, which significantly increased the final grain weight (Figure 6A–6E). STTM technology holds great promise for use in crop breeding. Our previous research showed that the expression of dozens of miRNAs negatively correlates with rice grain weight and filling rate (Peng et al., 2013, 2014). Seed-specific knockdown of these miRNAs may promote the formation of bigger seeds, leading to increased crop productivity. Similarly, in the horticultural crop tomato we constitutively blocked miR396, which increased fruit productivity in STTM396 transgenic plants (Figure 8C–8E). In summary, STTM-triggered miRNA degradation may serve as a useful tool for improving the yield of cereal and horticultural crops.

Establishment of STTMJB to Visualize Altered Gene Networks in STTM Transgenic Lines

In this study, we developed STTMJB, which currently accepts STTM-related RNA-seq and small RNA-seq data. STTMJB displays upregulation of miRNA target genes as well as changes in potential downstream genes in networks that might be affected by the specific miRNAs (Supplemental Figure 12). STTMJB also displays the specific downregulation of miRNAs targeted by STTM and how the levels of other miRNAs are affected, allowing researchers to glean information about potential regulatory relationships among miRNAs.

METHODS

Plant Material and Growth Conditions

The *A. thaliana* accession Columbia-0 (Col-0) and the tomato ecotype Micro-tom were used. All plants were grown in long-day conditions under a 16 h light/8 h dark cycle at 23°C. For the monocot plants *Oryza sativa* ssp. *Japonica* cv Nipponbare and *Zea mays*, the inbred line B104 served as the control for genetic transformation. Both WT and

transgenic plants were cultivated in a greenhouse under natural growing conditions with strict quarantine.

STTM Construction

Most STTMs were constructed by following the procedures described by Tang et al. (2012) and Teotia et al. (2017). In brief, specific STTM primers were designed and synthesized by Integrated DNA Technologies. The STTM fragment was introduced into the pOT2-Poly-Cis vector by PCR with the aid of SwaI sites on the primers for self-ligation, resulting in pOT2-STTM. The primers used to generate the STTMs in pOT2-Poly-Cis are listed in Supplemental Table 11. Alternatively, some STTMs were generated by chemical synthesis at Sangon Biotech (Supplemental Table 11). The pOT2-STTM vector was then used as a template in origin deletion PCR using primers containing PacI sites, generating the STTM-Cm^R (chloramphenicol) fragment with PacI sites on both ends. The STTM-Cm^R fragment together with pFGC5941-PacI (for *Arabidopsis*) or pCAMBIA1301-PacI (for rice and tomato) binary vectors were cleaved with PacI (NEB) and then ligated. The pFGC5941-STTM and pCAMBIA1301-STTM plasmids were transformed into DH5α, and positive transformants were selected on Luria–Bertani plates containing 25 mg/ml chloramphenicol and 50 mg/ml kanamycin (Sigma-Aldrich). For maize STTM construction, TF101.1 binary vector provided by Dr. Kang Wang at Iowa State University, was used instead of pFGC5941-PacI. In brief, the TF101.1 vector was introduced with PacI restriction site through the ligation of XbaI-to-SmaI fragment digested from pFGC5941-PacI vector, creating TF101.1-PacI. The remaining procedure was identical to that for the construction of pFGC5941-STTM and pCAMBIA1301-STTM. All final constructs were verified by sequencing.

For construction of tissue-specific STTMs in rice, the Gt13a promoter (He et al., 2011) and the pCAMBIA1301 binary vector were used in place of the enhanced *35S* promoter and the other binary vectors, respectively. *Agrobacterium* strain EHA105 was used for rice transformation.

For construction of inducible STTM165/166, the ~96-bp STTM region was amplified from the pFGC5941-STTM165/166 construct with primers containing AscI and PacI sites. The resulting PCR fragment was digested with AscI and PacI, and the digested fragment was cloned into the pER8 vector (Zuo et al., 2000) at the AscI–PacI sites. Expression was induced by continuous application of β-estradiol for several days. Specifically, 5-day-old seedlings were placed on MS medium containing β-estradiol to allow the phenotype to develop before taking pictures.

Plant Transformation and Screening for Transgenic Lines

The traditional flower-dipping method was used to transform *Arabidopsis* plants (Clough and Bent, 1998). Transgenic *Arabidopsis* lines were selected by spraying them with 0.1% glufosinate (bar herbicide). Rice transformation was performed following a previously published method (Teotia et al., 2017). Tomato transformation was performed as previously described (Jia et al., 2015), with the following modifications: we used hygromycin for transgenic selection based on the plasmid we used; only zeatin (ZT) was used for callus development, and ZT and gibberellic acid were applied for shoot development. Finally, we used Indolebutyric acid for root generation. Maize transformation was conducted by Dr. Kang Wang at Iowa State University. At least 10 lines of T1 or T2, heterozygous or homozygous transgenic plants were obtained for every STTM construct. At least 10 transgenic lines, for example STTM159, were used for analysis in each case, and only the lines showing consistent phenotypes were selected for further studies. Segregation ratios of these lines did not indicate the presence of multiple insertions.

Northern Blot Analysis

The same batch of total RNA used for qRT–PCR was used for northern blot analysis to validate the gene expression levels. In brief, a 15% urea PAGE gel was made from urea gel concentrate, urea diluent, and urea gel buffer (National Diagnostics). 10% Ammonium Persulfate (APS; 800 μl) (Fisher) and 40 μl of TEMED (Fisher) were added per 100 ml of gel mixture to polymerize the gel. A minimum of 10 μg of RNA sample was loaded and resolved on the 15% urea PAGE gel at 20 W for 2 h. RNA samples were transferred from the gel to nitrocellulose membrane (Bio-Rad) using a semi-dry transfer apparatus (Bio-Rad). Specific northern blot probes were labeled with γ-ATP^{32} (MP) and hybridized with the membrane. The images were collected with a phosphor imager (Fuji Film). Probe sequences can be found in Supplemental Table 11.

Small RNA Deep Sequencing, RNA-Seq, and Differential Expression Analyses

Total RNA extracted from three biological samples of each STTM transgenic *Arabidopsis* line and the control Col-0 plants collected at the initial flowering stage were used for small RNA-seq and RNA-seq. Small RNA sequencing was performed as described previously (Peng et al., 2011). In brief, small RNAs were first isolated by polyacrylamide/urea gel electrophoresis, then the 3′ Solexa DNA adaptor was ligated to the purified small RNAs, followed by 5′ Solexa RNA adaptor ligation. Purified small RNA products were then reverse transcribed and amplified by PCR. The resulting small RNA library was sequenced on the Genome Analyzer (Illumina) according to the manufacturer's instructions. After removing the adapter and low-quality sequences from the raw small RNA-seq data, the clean reads were directly aligned to the *Arabidopsis* miRNA precursors deposited in miRBase 19 using BLAST. The expression levels of specific miRNAs were calculated based on the abundance of mature miRNAs in the library. Normalization was performed using the following normalization formula: Normalized expression = actual miRNA count/total count of clean reads × 1 000 000. The normalized expression levels of known miRNAs was then used for differential expression analysis performed as described previously (Peng et al., 2011).

In brief, total RNAs isolated from STTM156/157, STTM165/166, STTM172 and control plants were digested by DNaseI and purified using oligo-dT beads to remove genomic DNA. Poly(A)-containing mRNAs were then fragmented into 130 bp followed by first-strand and second-strand cDNA synthesis. Purified cDNAs were end repaired and A-tails were added. This was followed by bubble adaptor ligation, PCR amplification, heat separation, single-strand cDNA circling, and rolling circle amplification, after which the purified products were sequenced. Fifty-bp length reads were sequenced using the BGISEQ-500 sequence platform at Beijing Genomics Institute (BGI, Shenzhen, China). After sequencing, tags were counted using the BGISEQ-500 Pipeline, which removed the reads with adaptors, reads with more than 5% unknown bases, and low-quality reads. The clean tags were mapped to the *Arabidopsis* genome (TAIR 10) using HISAT (Hierarchical Indexing for Spliced Alignment of Transcripts). When multiple expression reads were aligned to different regions of the same gene, expression levels were represented by the summation of all. The final gene expression data (clean reads) were normalized to RPKM (Reads Per Kilobase of transcript per Million mapped reads). Bioinformatics analysis was performed with the help of BGI Co. Ltd., China.

Quantitative Real-Time PCR for Gene Expression Studies

After transformation, three T1 transgenic lines with or without phenotypes were selected for expression assays of the miRNAs and their target genes. For *Arabidopsis*, the upper parts or the entire above-ground portions of transgenic plants were harvested at 23 days after germination for total RNA isolation using TRIzol (Invitrogen). Stem-loop real-time qRT–PCR was used to measure the miRNA expression levels and traditional qRT–PCR was used to determine the expression levels of miRNA target genes. *ACTIN* was used as an endogenous control for normalization, and WT was used as a sample control. The data thus obtained were analyzed by the $2^{-\Delta\Delta CT}$ method (Livak and Schmittgen, 2001).

Plant Electrophysiology

A. thaliana (WT and STTM165/166) plants were grown in soil under a 14 h light/ 10 h dark photoperiod and watered every 2 days. The humidity was

70%, and the temperatures were 22°C (day) and 18°C (night). For surface potential recording, 3- to 4-week-old plants were used. The protoplast isolation method has been described previously (Lemtiri-Chlieh and Berkowitz, 2004). After protoplast isolation, 20 μl of protoplasts was placed in a 2-ml chamber. The bath solution was used to record ABA-induced ICa (Murata et al., 2001). NADPH (5 mM) was freshly added to pipette solution. ABA stock solutions (5 mM) were stored in aliquots of 20 μl and were added to the bath solution to 50 μM using a pipette when ABA was needed. The osmolality of solutions was adjusted to 485 mOsm/kg (bath) and 500 mOsm/kg (pipette) with sorbitol.

Simultaneous signal recordings, voltage commands, and analyses were done using a microcomputer connected to the amplifier. After gigaohm seals were formed and whole-cell disposition was achieved, the membrane was clamped to a −30 mV holding potential. Liquid junction potentials were corrected. The standard voltage protocol ramped from 50 mV to −200 mV in 2 s. In all experiments, there was a waiting time of 3–5 min following whole-cell configuration before starting any current measurements. There was a wait time of 5–10 min after ABA was added to bath solution before starting to record currents for the same protoplast.

Development of the STTMJB Web Portal Using JBrowse to Display RNA-Seq and Small RNA-Seq Data

To develop the STTMJB web portal for visualizing genome-wide RNA- and small RNA-seq data from STTM transgenic lines, we downloaded and installed JBrowse (http://jbrowse.org/) (Skinner et al., 2009). We then followed the following procedures to set up JBrowse and prepare the sequencing data for visualization.

(1) Installation of the JBrowse server: JBrowse software was downloaded from http://jbrowse.org/. Thereafter, the uncompressed files were transferred to the designated directory (e.g./var/www/html) in the web server in a Linux or MacOS operating system. To install the prerequisite perl modules, the system administrator ran a script called setup.sh to configure the JBrowser system.

(2) Preparation of feature tracks and annotation files: the latest *A. thaliana* genome assembly, TAIR10 (*Arabidopsis*_167_TAIR9.fa), and compatible gene features (Athaliana_167_TAIR10.gene.gff3) were downloaded from Phytozome (https://phytozome.jgi.doe.gov/pz/portal.html). The following script in Jbrowse/bin directory was then executed to create a data folder in the directory called *Arabidopsis*; the command line is: $ bin/prepare-refseqs.pl –fasta./Athaliana_167.fa. JBrowse enables a search with a gene ID for quick visualization of the aligned reads surrounding the specific gene. To realize such functionality, the following script was executed using the GFF file: $ bin/flatfile-to-json.pl –gff Athaliana_167_TAIR10.gene.gff3 –tracklabel AT_GFF, where AT_GFF is the label we gave. To visualize small RNA-seq data, the small RNA GFF file called ath.gff3, which is compatible with *Arabidopsis*_167_TAIR9.fa and the TAIR10 annotation, was obtained from http://www.mirbase.org/ftp.shtml. This GFF file was also processed using the same aforementioned commands.

(3) Generation of BAM files from FASTQ sample data sets: BAM files are compatible file types in binary format representing SAM (Sequence Alignment) data in the JBrowse platform. We first used "Bowtie two" software to create indices required for alignment of reads to the *Arabidopsis* genome. We then used TopHat and Bowtie to align the reads from RNA-seq experiments, and the reads from small RNA-seq experiments, respectively, to the *Arabidopsis* genome. The resulting BAM files for each sample can be directly displayed by JBrowse without further preprocessing.

(4) Generation of BAM index files for JBrowse: to display the BAM file of each sample in a track in STTMJB, a companion index file was generated for each BAM file using the software package SAMtools. This index file has an extension of ".bam.bai," which allowed JBrowse to jump directly to any BAM file location without reading from the beginning.

(5) Loading of BAM files and their compatible index files into the web server and configuring JBrowser for visualization: after the BAM file and BAM index file for each sample were prepared, they were uploaded to the server where the files were reachable from the web server directory. The track configure file was prepared based on the locations of all BAM files and the track type required.

(6) Generation of the snapshots of specific gene expression patterns using STTMJB: to generate the snapshots of read alignments to a gene, we selected a specific region containing the gene and corresponding read alignments in one or multiple tracks, each representing a sample, and then took a screenshot of the selected region. Supplemental Figure 12 was generated in this fashion.

SUPPLEMENTAL INFORMATION

Supplemental Information is available at *Molecular Plant Online*.

FUNDING

This work was supported by the National Science Foundation, USA (IOS-1048216 and IOS-1340001), the National Natural Science Foundation of China (31571679, 31501292, 31871554), the Major Science and Technology Project of Henan Province (141100110600), the Support Plan of Science and Technology Innovation Team in Universities of Henan Province (17IRTSTHN015), and the Key Scientific Research Project in Universities of Henan Province (16A210009). G.T. is also supported by the Guangdong Innovation Research Team Fund (2014ZT05S078) and the 111 Project (D16014) to Henan University. S.T. was supported by a post-doctoral fellowship from Henan Agricultural University. F.M. was a visiting scholar supported by the China Scholarship Council (CSC). T.P., Z.Z., L.S., and L.T. were visiting PhD students supported by scholarships from Henan Agricultural University.

AUTHOR CONTRIBUTIONS

Conceptualization, G.T. and X.C.; Methodology, G.T., H.W., T.P., M.Q., H.L., S.T., and Z.Z.; Investigation, T.P., M.Q., H.L., S.T., Z.Z., Y.Z., B.W., D.Z., L.S., C.Z., B.L., K.R., Y.G., L.T., F.M., T.L. and L.H.; Formal Analysis, C.G., H.D., J.N., J.Q., T.P., and S.T.; Writing – Original Draft, T.P., S.T., and G.T.; Writing – Review & Editing, S.T., G.T., T.P., X.C., H.W., and X.T.; Visualization, T.P., S.T., and D.Z.; Data Curation, C.G. and H.W.; Funding Acquisition, G.T., Q.Z., and T.P.; Resources, Q.C., G.W., J.T., X.T., H.W., Q.Z., and G.T.; Supervision, G.T., X.C., Q.Z., and H.W.

ACKNOWLEDGMENTS

We are thankful to anonymous reviewers for their valuable suggestions for improving this article. No conflict of interest declared.

Received: September 18, 2017
Revised: August 1, 2018
Accepted: September 6, 2018
Published: September 19, 2018

REFERENCES

Allen, R.S., Li, J., Stahle, M.I., Dubroue, A., Gubler, F., and Millar, A.A. (2007). Genetic analysis reveals functional redundancy and the major target genes of the *Arabidopsis* miR159 family. Proc. Natl. Acad. Sci. USA **104**:16371–16376.

Bao, D., Ganbaatar, O., Cui, X., Yu, R., Bao, W., Falk, B.W., and Wuriyanghan, H. (2018). Down-regulation of genes coding for core RNAi components and disease resistance proteins via corresponding microRNAs might be correlated with successful Soybean mosaic virus infection in soybean. Mol. Plant Pathol. **19**:948–960.

Bian, H., Xie, Y., Guo, F., Han, N., Ma, S., Zeng, Z., Wang, J., Yang, Y., and Zhu, M. (2012). Distinctive expression patterns and roles of the miRNA393/TIR1 homolog module in regulating flag leaf inclination and primary and crown root growth in rice (*Oryza sativa*). New Phytol. **196**:149–161.

Brandt, R., Salla-Martret, M., Bou-Torrent, J., Musielak, T., Stahl, M., Lanz, C., Ott, F., Schmid, M., Greb, T., Schwarz, M., et al. (2012). Genome-wide binding-site analysis of REVOLUTA reveals a link between leaf patterning and light-mediated growth responses. Plant J. **72**:31–42.

Bouche, F., Lobet, G., Tocquin, P., and Perilleux, C. (2016). FLOR-ID: an interactive database of flowering-time gene networks in *Arabidopsis thaliana*. Nucleic Acids Res. **44**:D1167–D1171.

Cao, D., Wang, J., Ju, Z., Liu, Q., Li, S., Tian, H., Fu, D., Zhu, H., Luo, Y., and Zhu, B. (2016). Regulations on growth and development in tomato cotyledon, flower and fruit via destruction of miR396 with short tandem target mimic. Plant Sci. **247**:1–12.

Che, R., Tong, H., Shi, B., Liu, Y., Fang, S., Liu, D., Xiao, Y., Hu, B., Liu, L., Wang, H., et al. (2015). Control of grain size and rice yield by GL2-mediated brassinosteroid responses. Nat. plants **2**:15195.

Chen, Z.H., Bao, M.L., Sun, Y.Z., Yang, Y.J., Xu, X.H., Wang, J.H., Han, N., Bian, H.W., and Zhu, M.Y. (2011). Regulation of auxin response by miR393-targeted transport inhibitor response protein 1 is involved in normal development in *Arabidopsis*. Plant Mol. Biol. **77**:619–629.

Chuck, G., Meeley, R., and Hake, S. (2008). Floral meristem initiation and meristem cell fate are regulated by the maize AP2 genes ids1 and sid1. Development **135**:3013–3019.

Clough, S.J., and Bent, A.F. (1998). Floral dip: a simplified method for *Agrobacterium*-mediated transformation of *Arabidopsis thaliana*. Plant J. **16**:735–743.

Cui, J., You, C., and Chen, X. (2016). The evolution of microRNAs in plants. Curr. Opin. Plant Biol. **35**:61–67.

Duan, P., Ni, S., Wang, J., Zhang, B., Xu, R., Wang, Y., Chen, H., Zhu, X., and Li, Y. (2015). Regulation of OsGRF4 by OsmiR396 controls grain size and yield in rice. Nat. Plants **2**:15203.

Ebert, M.S., Neilson, J.R., and Sharp, P.A. (2007). MicroRNA sponges: competitive inhibitors of small RNAs in mammalian cells. Nat. Methods **4**:721–726.

Fei, Q., Li, P., Teng, C., and Meyers, B.C. (2015). Secondary siRNAs from Medicago NB-LRRs modulated via miRNA-target interactions and their abundances. Plant J. **83**:451–465.

Feng, S., Xu, Y., Guo, C., Zheng, J., Zhou, B., Zhang, Y., Ding, Y., Zhang, L., Zhu, Z., Wang, H., et al. (2016). Modulation of miR156 to identify traits associated with vegetative phase change in tobacco (*Nicotiana tabacum*). J. Exp. Bot. **67**:1493–1504.

Friml, J., Vieten, A., Sauer, M., Weijers, D., Schwarz, H., Hamann, T., Offringa, R., and Jurgens, G. (2003). Efflux-dependent auxin gradients establish the apical-basal axis of *Arabidopsis*. Nature **426**:147–153.

Franco-Zorrilla, J.M., Valli, A., Todesco, M., Mateos, I., Puga, M.I., Rubio-Somoza, I., Leyva, A., Weigel, D., Garcia, J.A., and Paz-Ares, J. (2007). Target mimicry provides a new mechanism for regulation of microRNA activity. Nat. Genet. **39**:1033–1037.

Fromm, B., Billipp, T., Peck, L.E., Johansen, M., Tarver, J.E., King, B.L., Newcomb, J.M., Sempere, L.F., Flatmark, K., Hovig, E., et al. (2015). A uniform system for the annotation of vertebrate microRNA genes and the evolution of the human microRNAome. Annu. Rev. Genet. **49**:213–242.

Fujii, H., Chiou, T.J., Lin, S.I., Aung, K., and Zhu, J.K. (2005). A miRNA involved in phosphate-starvation response in *Arabidopsis*. Curr. Biol. **15**:2038–2043.

Gao, F., Wang, K., Liu, Y., Chen, Y., Chen, P., Shi, Z., Luo, J., Jiang, D., Fan, F., Zhu, Y., et al. (2015). Blocking miR396 increases rice yield by shaping inflorescence architecture. Nat. Plants **2**:15196.

Gao, J., Chen, H., Yang, H., He, Yong., Tian, Z., and Li, J. (2018). A brassinosteroid responsive miRNA-target module regulates gibberellin biosynthesis and plant development. New Phytol. **220**:488–501.

Gou, J.Y., Felippes, F.F., Liu, C.J., Weigel, D., and Wang, J.W. (2011). Negative regulation of anthocyanin biosynthesis in *Arabidopsis* by a miR156-targeted SPL transcription factor. Plant Cell **23**:1512–1522.

Gu, Z., Huang, C., Li, F., and Zhou, X. (2014). A versatile system for functional analysis of genes and microRNAs in cotton. Plant Biotechnol. J. **12**:638–649.

Guo, G., Liu, X., Sun, F., Cao, J., Huo, N., Wuda, B., Xin, M., Hu, Z., Du, J., Xia, R., et al. (2018). Wheat miR9678 affects seed germination by generating phased siRNAs and modulating abscisic acid/gibberellin signaling. Plant Cell **30**:796–814.

He, Y., Ning, T., Xie, T., Qiu, Q., Zhang, L., Sun, Y., Jiang, D., Fu, K., Yin, F., Zhang, W., et al. (2011). Large-scale production of functional human serum albumin from transgenic rice seeds. Proc. Natl. Acad. Sci. USA **108**:19078–19083.

Jia, X.Y., Ding, N., Fan, W.X., Yan, J., Gu, Y.Y., Tang, X.Q., Li, R.Z., and Tang, G.L. (2015). Functional plasticity of miR165/166 in plant development revealed by small tandem target mimic. Plant Sci. **233**:11–21.

Jian, C., Han, R., Chi, Q., Wang, S., Ma, M., Liu, X., and Zhao, H. (2017). Virus-based microRNA silencing and overexpressing in common wheat (*Triticum aestivum* L.). Front. Plant Sci. **8**:500.

Jiang, N., Meng, J., Cui, J., Sun, G., and Luan, Y. (2018). Function identification of miR482b, a negative regulator during tomato resistance to *Phytophthora infestans*. Hortic. Res. **5**:9.

Jiao, Y., Wang, Y., Xue, D., Wang, J., Yan, M., Liu, G., Dong, G., Zeng, D., Lu, Z., Zhu, X., et al. (2010). Regulation of OsSPL14 by OsmiR156 defines ideal plant architecture in rice. Nat. Genet. **42**:541–544.

Jones-Rhoades, M.W., and Bartel, D.P. (2004). Computational identification of plant microRNAs and their targets, including a stress-induced miRNA. Mol. Cell **14**:787–799.

Kawashima, C.G., Matthewman, C.A., Huang, S., Lee, B.R., Yoshimoto, N., Koprivova, A., Rubio-Somoza, I., Todesco, M., Rathjen, T., Saito, K., et al. (2011). Interplay of SLIM1 and miR395 in the regulation of sulfate assimilation in *Arabidopsis*. Plant J. **66**:863–876.

Kawashima, C.G., Yoshimoto, N., Maruyama-Nakashita, A., Tsuchiya, Y.N., Saito, K., Takahashi, H., and Dalmay, T. (2009). Sulphur starvation induces the expression of microRNA-395 and one of its target genes but in different cell types. Plant J. **57**:313–321.

Kim, J.J., Lee, J.H., Kim, W., Jung, H.S., Huijser, P., and Ahn, J.H. (2012). The microRNA156-SQUAMOSA PROMOTER BINDING PROTEIN-LIKE3 module regulates ambient temperature-responsive flowering via FLOWERING LOCUS T in *Arabidopsis*. Plant Physiol. **159**:461–478.

Lan, Y., Su, N., Shen, Y., Zhang, R., Wu, F., Cheng, Z., Wang, J., Zhang, X., Guo, X., and Lei, C. (2012). Identification of novel MiRNAs and MiRNA expression profiling during grain development in indica rice. BMC Genomics **13**:264.

Lemtiri-Chlieh, F., and Berkowitz, G.A. (2004). Cyclic adenosine monophosphate regulates calcium channels in the plasma membrane of *Arabidopsis* leaf guard and mesophyll cells. J. Biol. Chem. **279**:35306–35312.

Lewis, B.P., Shih, I.H., Jones-Rhoades, M.W., Bartel, D.P., and Burge, C.B. (2003). Prediction of mammalian microRNA targets. Cell **115**:787–798.

Li, J., Reichel, M., Li, Y., and Millar, A.A. (2014). The functional scope of plant microRNA-mediated silencing. Trends Plant Sci. **19**:750–756.

Li, S., Gao, F., Xie, K., Zeng, X., Cao, Y., Zeng, J., He, Z., Ren, Y., Li, W., Deng, Q., et al. (2016). The OsmiR396c-OsGRF4-OsGIF1 regulatory

module determines grain size and yield in rice. Plant Biotechnol. J. **14**:2134–2146.

Liu, B., Zhang, J., Yang, S., Ji, K., Liu, X., Du, B., Jia, Q., Qi, S., Li, X., and Fan, R. (2018). Effect of silencing microRNA-508 by STTM on melanogenesis in alpaca (*Vicugna pacos*). Gene https://doi.org/10.1016/j.gene.2018.08.011.

Liu, J., Cheng, X., Liu, D., Xu, W., Wise, R., and Shen, Q.H. (2014). The miR9863 family regulates distinct Mla alleles in barley to attenuate NLR receptor-triggered disease resistance and cell-death signaling. PLoS Genet. **10**:e1004755.

Liu, Z., Jia, L., Wang, H., and He, Y. (2011). HYL1 regulates the balance between adaxial and abaxial identity for leaf flattening via miRNA-mediated pathways. J. Exp. Bot. **62**:4367–4381.

Livak, K.J., and Schmittgen, T.D. (2001). Analysis of relative gene expression data using real-time quantitative PCR and the 2(-Delta Delta C(T)) method. Methods **25**:402–408.

Mashiguchi, K., Tanaka, K., Sakai, T., Sugawara, S., Kawaide, H., Natsume, M., Hanada, A., Yaeno, T., Shirasu, K., Yao, H., et al. (2011). The main auxin biosynthesis pathway in *Arabidopsis*. Proc. Natl. Acad. Sci. USA **108**:18512–18517.

McCue, A.D., Nuthikattu, S., and Slotkin, R.K. (2013). Genome-wide identification of genes regulated in trans by transposable element small interfering RNAs. RNA Biol. **10**:1379–1395.

Miura, K., Ikeda, M., Matsubara, A., Song, X.J., Ito, M., Asano, K., Matsuoka, M., Kitano, H., and Ashikari, M. (2010). OsSPL14 promotes panicle branching and higher grain productivity in rice. Nat. Genet. **42**:545–549.

Murata, Y., Pei, Z.M., Mori, I.C., and Schroeder, J. (2001). Abscisic acid activation of plasma membrane Ca(2+) channels in guard cells requires cytosolic NAD(P)H and is differentially disrupted upstream and downstream of reactive oxygen species production in abi1-1 and abi2-1 protein phosphatase 2C mutants. Plant Cell **13**:2513–2523.

Peng, T., Lv, Q., Zhang, J., Li, J., Du, Y., and Zhao, Q. (2011). Differential expression of the microRNAs in superior and inferior spikelets in rice (*Oryza sativa*). J. Exp. Bot. **62**:4943–4954.

Peng, T., Sun, H., Du, Y., Zhang, J., Li, J., Liu, Y., Zhao, Y., and Zhao, Q. (2013). Characterization and expression patterns of microRNAs involved in rice grain filling. PLoS One **8**:e54148.

Peng, T., Sun, H., Qiao, M., Zhao, Y., Du, Y., Zhang, J., Li, J., Tang, G., and Zhao, Q. (2014). Differentially expressed microRNA cohorts in seed development may contribute to poor grain filling of inferior spikelets in rice. BMC Plant Biol. **14**:196.

Proust, H., Bazin, J., Sorin, C., Hartmann, C., Crespi, M., and Lelandais-Briere, C. (2018). Stable inactivation of MicroRNAs in *Medicago truncatula* roots. Methods Mol. Biol. **1822**:123–132.

Reichel, M., Li, Y., Li, J., and Millar, A.A. (2015). Inhibiting plant microRNA activity: molecular SPONGEs, target MIMICs and STTMs all display variable efficacies against target microRNAs. Plant Biotechnol. J. **13**:915–926.

Rubio-Somoza, I., and Weigel, D. (2011). MicroRNA networks and developmental plasticity in plants. Trends Plant Sci. **16**:258–264.

Rubio-Somoza, I., and Weigel, D. (2013). Coordination of flower maturation by a regulatory circuit of three microRNAs. PLoS Genet. **9**:e1003374.

Sarvepalli, K., and Nath, U. (2011). Hyper-activation of the TCP4 transcription factor in *Arabidopsis thaliana* accelerates multiple aspects of plant maturation. Plant J. **67**:595–607.

Schommer, C., Bresso, E., Spinelli, S., and Palatnik, J. (2012). Role of microRNA miR319 in plant development. In MicroRNAs in Plant Development and Stress Responses, R. Sunkar, ed. (Berlin Heidelberg: Springer), pp. 29–47.

Sha, A.H., Zhao, J.P., Yin, K.Q., Tang, Y., Wang, Y., Wei, X., Hong, Y.G., and Liu, Y.L. (2014). Virus-based microRNA silencing in plants. Plant Physiol. **164**:36–47.

Si, L., Chen, J., Huang, X., Gong, H., Luo, J., Hou, Q., Zhou, T., Lu, T., Zhu, J., Shangguan, Y., et al. (2016). OsSPL13 controls grain size in cultivated rice. Nat. Genet. **48**:447–456.

Skinner, M.E., Uzilov, A.V., Stein, L.D., Mungall, C.J., and Holmes, I.H. (2009). JBrowse: a next-generation genome browser. Genome Res. **19**:1630–1638.

Sosa-Valencia, G., Palomar, M., Covarrubias, A.A., and Reyes, J.L. (2017). The legume miR1514a modulates a NAC transcription factor transcript to trigger phasiRNA formation in response to drought. J. Exp. Bot. **68**:2013–2026.

Su, Y., Li, H.G., Wang, Y., Li, S., Wang, H.L., Yu, L., He, F., Yang, Y., Feng, C.H., Shuai, P., et al. (2018). Poplar miR472a targeting NBS-LRRs is involved in effective defense response to necrotrophic fungus *Cytospora chrysosperma*. J. Exp. Bot. https://doi.org/10.1093/jxb/ery304.

Sun, P., Zhang, W., Wang, Y., He, Q., Shu, F., Liu, H., Wang, J., Yuan, L., and Deng, H. (2016). OsGRF4 controls grain shape, panicle length and seed shattering in rice. J. Integr. Plant Biol. **58**:836–847.

Tan, B.C., Schwartz, S.H., Zeevaart, J.A., and McCarty, D.R. (1997). Genetic control of abscisic acid biosynthesis in maize. Proc. Natl. Acad. Sci. USA **94**:12235–12240.

Tang, G., Yan, J., Gu, Y., Qiao, M., Fan, R., Mao, Y., and Tang, X. (2012). Construction of short tandem target mimic (STTM) to block the functions of plant and animal microRNAs. Methods **58**:118–125.

Tang, G.L. (2010). Plant microRNAs: an insight into their gene structures and evolution. Semin. Cell Dev. Biol. **21**:782–789.

Taylor, I.B., Burbidge, A., and Thompson, A.J. (2000). Control of abscisic acid synthesis. J. Exp. Bot. **51**:1563–1574.

Teotia, S., Singh, D., Tang, X., and Tang, G. (2016). Essential RNA-based technologies and their applications in plant functional genomics. Trends Biotechnol. **34**:106–123.

Teotia, S., and Tang, G. (2015). To bloom or not to bloom: role of microRNAs in plant flowering. Mol. Plant **8**:359–377.

Teotia, S., Zhang, D., and Tang, G. (2017). Knockdown of rice microRNA166 by short tandem target mimic (STTM). Methods Mol. Biol. **1654**:337–349.

Teotia, S., and Tang, G. (2017). Silencing of stress-regulated miRNAs in plants by short tandem target mimic (STTM) approach. Methods Mol. Biol. **1631**:337–348.

Todesco, M., Rubio-Somoza, I., Paz-Ares, J., and Weigel, D. (2010). A collection of target mimics for comprehensive analysis of microRNA function in *Arabidopsis thaliana*. PLoS Genet. **6**:e1001031.

Wang, G., Jiang, H., Del Toro de Leon, G., Martinez, G., and Kohler, C. (2018). Sequestration of a transposon-derived siRNA by a target mimic imprinted gene induces postzygotic reproductive isolation in *Arabidopsis*. Dev. Cell https://doi.org/10.1016/j.devcel.2018.07.014.

Wang, S.-t., Sun, X.-l., Hoshino, Y., Yu, Y., Jia, B., Sun, Z.-w., Sun, M.-z., Duan, X.-b., and Zhu, Y.-m. (2014). MicroRNA319 positively regulates cold tolerance by targeting OsPCF6 and OsTCP21 in rice (*Oryza sativa* L.). PLoS One **9**:e91357.

Wang, S., Wu, K., Yuan, Q., Liu, X., Liu, Z., Lin, X., Zeng, R., Zhu, H., Dong, G., Qian, Q., et al. (2012). Control of grain size, shape and quality by OsSPL16 in rice. Nat. Genet. **44**:950–954.

Wong, J., Gao, L., Yang, Y., Zhai, J.X., Arikit, S., Yu, Y., Duan, S.Y., Chan, V., Xiong, Q., Yan, J., et al. (2014). Roles of small RNAs in soybean defense against *Phytophthora sojae* infection. Plant J. **79**:928–940.

Wu, G., Park, M.Y., Conway, S.R., Wang, J.W., Weigel, D., and Poethig, R.S. (2009). The sequential action of miR156 and miR172 regulates developmental timing in *Arabidopsis*. Cell **138**:750–759.

Xia, K., Wang, R., Ou, X., Fang, Z., Tian, C., Duan, J., Wang, Y., and Zhang, M. (2012). OsTIR1 and OsAFB2 downregulation via OsmiR393 overexpression leads to more tillers, early flowering and less tolerance to salt and drought in rice. PLoS One **7**:e30039.

Xia, K., Zeng, X., Jiao, Z., Li, M., Xu, W., Nong, Q., Mo, H., Cheng, T., and Zhang, M. (2018). Formation of protein disulfide bonds catalyzed by OsPDIL1;1 is mediated by MicroRNA5144-3p in rice. Plant Cell Physiol. **59**:331–342.

Xu, M.Y., Zhang, L., Li, W.W., Hu, X.L., Wang, M.B., Fan, Y.L., Zhang, C.Y., and Wang, L. (2014). Stress-induced early flowering is mediated by miR169 in *Arabidopsis thaliana*. J. Exp. Bot. **65**:89–101.

Yan, J., Gu, Y.Y., Jia, X.Y., Kang, W.J., Pan, S.J., Tang, X.Q., Chen, X.M., and Tang, G.L. (2012). Effective small RNA destruction by the expression of a short tandem target mimic in *Arabidopsis*. Plant Cell **24**:415–427.

Yan, J., Zhao, C., Zhou, J., Yang, Y., Wang, P., Zhu, X., Tang, G., Bressan, R.A., and Zhu, J.K. (2016). The miR165/166 mediated regulatory module plays critical roles in ABA homeostasis and response in *Arabidopsis thaliana*. PLoS Genet. **12**:e1006416.

Yang, L., Xu, M., Koo, Y., He, J., and Poethig, R.S. (2013). Sugar promotes vegetative phase change in *Arabidopsis thaliana* by repressing the expression of MIR156A and MIR156C. ELife **2**: e00260.

Yang, T., Wang, Y., Teotia, S., Zhang, Z., and Tang, G. (2018). The making of leaves: how small RNA networks modulate leaf development. Front. Plant Sci. **9**:824.

Yi, R., Zhu, Z., Hu, J., Qian, Q., Dai, J., and Ding, Y. (2013). Identification and expression analysis of microRNAs at the grain filling stage in rice (*Oryza sativa* L.) via deep sequencing. PLoS One **8**:e57863.

Yu, S., Cao, L., Zhou, C.M., Zhang, T.Q., Lian, H., Sun, Y., Wu, J., Huang, J., Wang, G., and Wang, J.W. (2013). Sugar is an endogenous cue for juvenile-to-adult phase transition in plants. ELife **2**:e00269.

Zhang, H., Zhang, J., Yan, J., Gou, F., Mao, Y., Tang, G., Botella, J.R., and Zhu, J.-K. (2017a). Short tandem target mimic rice lines uncover functions of miRNAs in regulating important agronomic traits. Proc. Natl. Acad. Sci. USA **114**:5277–5282.

Zhang, Q., Li, Y., Zhang, Y., Wu, C., Wang, S., Hao, L., Wang, S., and Li, T. (2017b). Md-miR156ab and Md-miR395 target WRKY transcription factors to influence apple resistance to leaf spot disease. Front. Plant Sci. **8**:526.

Zhang, J., Zhang, H., Srivastava, A.K., Pan, Y., Bai, J., Fang, J., Shi, H., and Zhu, J.K. (2018). Knockdown of rice microRNA166 confers drought resistance by causing leaf rolling and altering stem xylem development. Plant Physiol. **176**:2082–2094.

Zhao, Y., Peng, T., Sun, H., Teotia, S., Wen, H., Du, Y., Zhang, J., Li, J., Tang, G., Xue, H., et al. (2018). miR1432-OsACOT (Acyl-CoA thioesterase) module determines grain yield via enhancing grain filling rate in rice. Plant Biotechnol. J. https://doi.org/10.1111/pbi.13009.

Zhao, Y., Wen, H., Teotia, S., Du, Y., Zhang, J., Li, J., Sun, H., Tang, G., Peng, T., and Zhao, Q. (2017). Suppression of microRNA159 impacts multiple agronomic traits in rice (*Oryza sativa* L.). BMC Plant Biol. **17**:215.

Zhu, Q.H., Spriggs, A., Matthew, L., Fan, L., Kennedy, G., Gubler, F., and Helliwell, C. (2008). A diverse set of microRNAs and microRNA-like small RNAs in developing rice grains. Genome Res. **18**:1456–1465.

Zuo, J., and Li, J. (2014). Molecular genetic dissection of quantitative trait loci regulating rice grain size. Annu. Rev. Genet. **48**:99–118.

Zuo, J., Niu, Q.W., and Chua, N.H. (2000). Technical advance: an estrogen receptor-based transactivator XVE mediates highly inducible gene expression in transgenic plants. Plant J. **24**:265–273.